

1 **Large but decreasing effect of ozone on the European carbon**
2 **sink**

3 Rebecca J Oliver¹, Lina M Mercado^{1,2}, Stephen Sitch², David Simpson^{3,4}, Belinda E Medlyn⁵,
4 Yan-Shih Lin⁵, Gerd A Folberth⁶

5

6 ¹ Centre for Ecology and Hydrology, Benson Lane, Wallingford, OX10 8BB, UK

7 ² College of Life and Environmental Sciences, University of Exeter, EX4 4RJ, Exeter, UK

8 ³ EMEP MSC-W Norwegian Meteorological Institute, PB 43, NO-0313, Oslo, Norway

9 ⁴ Dept. Space, Earth & Environment, Chalmers University of Technology, Gothenburg, SE-41296 Sweden

10 ⁵ Hawkesbury Institute for the Environment, Western Sydney University, Locked Bag 1797, Penrith NSW 2751
11 Australia

12 ⁶ Met Office Hadley Centre, Exeter, UK.

13 *Correspondence to:* Rebecca Oliver (rfu@ceh.ac.uk)

14

15

16

17

18

19

20

21

22

23

24

25

26 **Abstract**

27

28 The capacity of the terrestrial biosphere to sequester carbon and mitigate climate change is governed by the ability
29 of vegetation to remove emissions of CO₂ through photosynthesis. Tropospheric O₃, a globally abundant and
30 potent greenhouse gas, is, however, known to damage plants, causing reductions in primary productivity. Despite
31 emission control policies across Europe, background concentrations of tropospheric O₃ have risen significantly
32 over the last decades due to hemispheric-scale increases in O₃ and its precursors. Therefore, plants are exposed to
33 increasing background concentrations, at levels currently causing chronic damage. Studying the impact of O₃ on
34 European vegetation at the regional scale is important for gaining greater understanding of the impact of O₃ on
35 the land carbon sink at large spatial scales. In this work we take a regional approach and update the JULES land-
36 surface model using new measurements specifically for European vegetation. Given the importance of stomatal
37 conductance in determining the flux of O₃ into plants, we implement an alternative stomatal closure
38 parameterization and account for diurnal variations in O₃ concentration in our simulations. We conduct our
39 analysis specifically for the European region to quantify the impact of the interactive effects of tropospheric O₃
40 and CO₂, and its interaction with CO₂, on gross primary productivity (GPP) and land carbon storage across Europe.
41 A factorial set of model experiments showed that tropospheric O₃ can suppress terrestrial carbon uptake across
42 Europe over the period 1901 to 2050. By 2050, simulated GPP was reduced by 4 to 9% due to plant O₃ damage
43 and land carbon storage by 3 to 7%. The combined physiological effects of elevated future CO₂ (acting to reduce
44 stomatal opening) and reductions in O₃ concentrations resulted in reduced O₃ damage in the future. This alleviation
45 of O₃ damage by CO₂ induced stomatal closure was around 1 to 2% for both land carbon and GPP, depending on
46 plant sensitivity to O₃ for low and high sensitivity respectively (on both land carbon and GPP). Reduced land
47 carbon storage resulted from diminished soil carbon stocks consistent with the reduction in GPP. Regional
48 variations are identified with larger impacts shown for temperate Europe (GPP reduced by 10 to 20%) compared
49 to boreal regions (GPP reduced by 2 to 8%). These results highlight that O₃ damage needs to be considered when
50 predicting GPP and land carbon, and that the effects of O₃ on plant physiology need to be considered in regional
51 land carbon cycle assessments.

52

53

54

55

56

57

58

59

60 1 Introduction

61

62 The terrestrial biosphere absorbs around 30% of anthropogenic CO₂ emissions and acts to mitigate climate change
63 (Le Quéré et al., 2015). Early estimates of the European carbon balance suggest a terrestrial carbon sink of between
64 135 to 205 TgC yr⁻¹ (Janssens et al., 2003). Schulze et al. (2009) determined a larger carbon sink of 274 TgC yr⁻¹,
65 and more recent estimates suggest a European terrestrial sink of between 146 to 184 TgC yr⁻¹ (Luysaert et al.,
66 2012). The carbon sink capacity of land ecosystems is dominated by the ability of vegetation to sequester carbon
67 through photosynthesis and release it back to the atmosphere through respiration. Therefore, any change in the
68 balance of these fluxes will alter ecosystem source-sink behaviour.

69

70 In recent decades much attention has focussed on the effects of rising atmospheric CO₂ on vegetation productivity
71 (Ceulemans and Mousseau, 1994;Norby et al., 2005;Norby et al., 1999;Saxe et al., 1998). The Norby et al. (2005)
72 synthesis of Free Air CO₂ Enrichment (FACE) experiments suggests a median stimulation (23 ± 2%) of forest
73 NPP in response to a doubling of CO₂. Similar average increases (20%) were observed for C₃ crops, although this
74 translated into smaller gains in biomass (17%) and crop yields (13%) (Long et al., 2006). Little attention, however,
75 has been given to tropospheric ozone (O₃), a globally abundant air pollutant recognised as one of the most
76 damaging pollutants for forests (Karlsson et al., 2007;Royal-Society, 2008;Simpson et al., 2014b). Tropospheric
77 O₃ is a secondary air pollutant formed by photochemical reactions involving carbon monoxide (CO), volatile
78 organic compounds (VOCs), methane (CH₄) and nitrogen oxides (NO_x) from both man-made and natural sources,
79 as well as downward transport from the stratosphere and lightning which is a source of NO_x. The phytotoxic
80 effects of O₃ exposure are shown to decrease vegetation productivity and biomass, with consequences for
81 terrestrial carbon sequestration (Felzer et al., 2004;Loya et al., 2003;Mills et al., 2011b;Sitch et al., 2007). Few
82 studies, however, consider the simultaneous effects of exposure to both gases, and few Earth-system models
83 (ESMs) currently explicitly consider the role of tropospheric O₃ in terrestrial carbon dynamics (IPCC, 2013), both
84 of which are important to understanding the carbon sequestration potential of the land-surface, and future carbon
85 dynamics regionally and globally (Le Quéré et al., 2016;Sitch et al., 2015).

86

87 Due to increased anthropogenic precursor emissions over the industrial period, background concentrations of
88 ground-level O₃ have risen (Vingarzan, 2004). Background O₃ is generally defined as the O₃ pollution present in
89 a region that is not attributed to local anthropogenic sources (Vingarzan, 2004). O₃ levels at the start of the 20th
90 century are estimated to be around 10 ppb for the site Montsouris Observatory near Paris, data for Arkona on the
91 Baltic coast increased from ca. 15 ppb in the 1950s to 20-27 ppb by the early 1980s, and the Irish coast site Mace
92 Head shows around 40 ppb by the year 2000 (Logan et al., 2012;Parrish et al., 2012). Present day annual average
93 background O₃ concentrations reported in the review of Vingarzan (2004) show O₃ concentrations range between
94 approximately 20 and 45 ppb, with the greatest increase occurring since the 1950s. Trends vary from site to site
95 though, even on a decadal basis (Logan et al., 2012;Simpson et al., 2014b), depending, for example, on
96 local/regional trends in precursor (especially NO_x) emissions, elevation, and exposure to long-range transport of
97 O₃. Nevertheless, there is some indication that background O₃ levels over the mid-latitudes of the Northern
98 Hemisphere have continued to rise at a rate of approximately 0.5–2% per year, although not uniform (Vingarzan,
99 2004). As a result of controls on precursor emissions in Europe and North America, peak O₃ concentrations in

100 these regions have decreased or stabilised over recent decades (Cooper et al., 2014; Logan et al., 2012; Parrish et
101 al., 2012; Simpson et al., 2014b). Nevertheless, climate change may increase the frequency of weather events
102 conducive to peak O₃ incidents in the future (e.g. summer droughts and heat-waves; e.g., (Sicard et al., 2013)),
103 and may increase biogenic emissions of the O₃-precursors isoprene and NO_x, although such impacts are subject
104 to great uncertainty (Simpson et al., 2014b; Young et al., 2013; Young et al., 2009). Intercontinental transport of
105 air pollution from regions such as Asia ~~that currently have poor emission controls~~ are thought to contribute
106 substantially to rising background O₃ concentrations over the last decades (Cooper et al., 2010; Verstraeten et al.,
107 2015). Northern Hemisphere background concentrations of O₃ are now close to established levels for impacts on
108 human health and the terrestrial environment (Royal-Society, 2008). Therefore, although peak O₃ concentrations
109 are in decline across Europe, plants are exposed to increasing background levels, at levels currently causing
110 chronic damage (Mills et al., 2011b). Intercontinental transport means future O₃ concentrations in Europe will be
111 partly dependent on how O₃ precursor emissions evolve globally (Auvray and Bey, 2005; Derwent et al., 2015).

112

113 ~~Rising background~~ Elevated O₃ concentrations impact agricultural yields and nutritional quality of major crops
114 (Ainsworth et al., 2012; Avnery et al., 2011), with consequences for global food security (Tai et al., 2014). ~~As well~~
115 ~~as being a significant air pollutant, O₃ is a potent greenhouse gas (Royal Society, 2008).~~ High Increasing
116 background levels of O₃ are damaging to ecosystem health and reduce the global land carbon sink (Arneeth et al.,
117 2010; Sitch et al., 2007). Reduced uptake of carbon by plant photosynthesis due to O₃ damage allows more CO₂
118 to remain in the atmosphere. This effect of O₃ on plant physiology represents an additional climate warming to
119 the direct radiative forcing of O₃, a potent greenhouse gas (Collins et al., 2010; Sitch et al., 2007), the magnitude
120 of which, however, remains highly uncertain (IPCC, 2013).

121

122 Dry deposition of O₃ to terrestrial surfaces, primarily uptake by stomata on plant foliage and deposition on external
123 surfaces of vegetation (Fowler et al., 2001; Fowler et al., 2009), is a large sink for ground level O₃ (Wild,
124 2007; Young et al., 2013). On entry to sub-stomatal spaces, O₃ reacts with other molecules to form reactive oxygen
125 species (ROS). Plants can tolerate a certain level of O₃ depending on their capacity to scavenge and detoxify the
126 ROS (Ainsworth et al., 2012). Above this critical level, long-term chronic O₃ exposure reduces plant
127 photosynthesis and biomass accumulation (Ainsworth, 2008; Ainsworth et al., 2012; Matyssek et al., 2010a; Wittig
128 et al., 2007; Wittig et al., 2009), either directly through effects on photosynthetic machinery such as reduced
129 Rubisco content (Ainsworth et al., 2012; Wittig et al., 2009) and/or indirectly by reduced stomatal conductance
130 (g_s) (Kitao et al., 2009; Wittig et al., 2007), alters carbon allocation to different pools (Grantz et al., 2006; Wittig
131 et al., 2009), accelerates leaf senescence (Ainsworth, 2008; Nunn et al., 2005; Wittig et al., 2009) and changes plant
132 susceptibility to biotic stress factors (Karnosky et al., 2002; Percy et al., 2002).

133

134 The response of plants to O₃ is very wide ranging as reported in the literature from different field studies. The
135 Wittig et al. (2007) meta-analysis of temperate and boreal tree species showed raised O₃ concentrations future
136 concentrations of O₃ predicted for 2050 significantly reduced leaf level light saturated net photosynthetic uptake
137 (-19%, range: -3% to -28% at a mean O₃ concentration of 85 ppb) and g_s (-10%, range: +5% to -23% at a mean
138 O₃ concentration of 91 ppb) in both broadleaf and needle leaf tree species. In the Feng et al. (2008) meta-analysis
139 of wheat, ~~projected O₃ concentrations for the future~~ reduced aboveground biomass (-18% at a mean O₃

140 concentration of 70 ppb) photosynthetic rate (-20% at a mean O₃ concentration of 73 ppb) and g_s (-22% at a mean
141 O₃ concentration of 79 ppb). One of few long-term field based O₃ exposure studies (AspenFACE) showed that
142 after 11 years of exposing mature trees to ~~elevated-O₃ concentrations~~ (mean O₃ concentration of 46 ppb), O₃
143 decreased ecosystem carbon content (-9%), and decreased NPP (-10%), although the O₃ effect decreased through
144 time (Talhelm et al., 2014). Zak et al. (2011) showed this was partly due to a shift in community structure as O₃-
145 tolerant species, competitively inferior in low O₃ environments, out competed O₃-sensitive species. GPP was
146 reduced (-12% to -19%) at two Mediterranean ecosystems exposed to ~~high ambient-O₃ concentrations~~ (ranging
147 between 20 to 72 ppb across sites and through the year) studied by Fares et al. (2013). Biomass of mature beech
148 trees was reduced (-44%) after 8 years of exposure to ~~elevated-O₃~~ (~150 ppb) (Matyssek et al., 2010a). After 5
149 years of O₃ exposure (ambient +20 to +40 ppb) in a semi-natural grassland, annual biomass production was
150 reduced (-23%), and in a Mediterranean annual pasture O₃ exposure significantly reduced total aboveground
151 biomass (up to -25%) (Calvete-Sogo et al., 2014). However, these were empirical studies at individual sites, and
152 these focus on O₃ effects on plant physiology and productivity, but do not quantify the impact on the land carbon
153 sink. Modelling studies are needed to scale site observations to the regional and global scales. Models generally
154 suggest that plant productivity and carbon sequestration will decrease with O₃ pollution, though the magnitudes
155 vary. For example, based on a limited dataset to parameterise plant O₃ damage for a global set of plant functional
156 types, Sitch et al. (2007) predicted a decline in global GPP of 14 to 23% by 2100. A second study by Lombardozzi
157 et al. (2015) ~~similarly~~ predicted a 10.8% decrease of ~~present-day (2002-2009) global~~ GPP globally. Here we take
158 a regional approach and take advantage of the latest measurements showing changes in plant productivity with
159 accumulated exposure to O₃ specifically for a range of European vegetation from different regions (CLRTAP
160 2017) with which to calibrate the JULES model for plant sensitivity to O₃, and conduct our analysis specifically
161 for the European region.

162

163 Understanding the response of plants to elevated tropospheric O₃ is challenged by the large variation in O₃
164 sensitivity both within and between species (Karnosky et al., 2007; Kubiske et al., 2007; Wittig et al., 2009).
165 Additionally, other environmental stresses that affect stomatal behaviour will affect the rate of O₃ uptake and
166 therefore the response to O₃ exposure, such as high temperature, drought and changing concentrations of
167 atmospheric CO₂ (Mills et al., 2016; Fagnano et al., 2009; Kitao et al., 2009; Löw et al., 2006). Increasing
168 concentrations of atmospheric CO₂, for example, are suggested to provide some protection against O₃ damage by
169 causing stomata to close (Harmens et al., 2007; Wittig et al., 2007), however the long-term effects of CO₂
170 fertilisation on plant growth and carbon storage remain uncertain (Baig et al., 2015; Ciais et al., 2013). Further, in
171 some studies, stomata have been shown to respond sluggishly, losing their responsiveness to environmental
172 stimuli with exposure to O₃ which can lead to higher O₃ uptake, increased water-loss and therefore greater
173 vulnerability to environmental stresses such as drought (Mills et al., 2016; Mills et al., 2009; Paoletti and Grulke,
174 2010; Wilkinson and Davies, 2009).

175

176 Given the critical role g_s plays in the uptake of both CO₂ and O₃, we use an alternative representation and
177 parameterisation of g_s in JULES by implementing the Medlyn *et al.* (2011) g_s formulation. This model is based
178 on the optimal theory of stomatal behaviour and has advantages over the current JULES g_s formulation of Jacobs
179 (1994) including i) a single parameter (g₁) compared to two parameters in Jacobs (1994), ii) the g₁ parameter is

180 related to the water-use strategy of vegetation and is easier to parameterise with commonly measured leaf or
181 canopy level observations of photosynthesis, g_s and humidity, and (iii) values of g_1 are available for many
182 different plant functional types (PFTs) derived from a global data set of leaf-level measurements (Lin et al., 2015).

183

184 The main objective of this work is to assess the impact of historical and projected (1901 to 2050) changes in
185 tropospheric O_3 and atmospheric CO_2 concentration on predicted GPP and the land-carbon sink for Europe.
186 These are the two greenhouse gases that directly affect plant photosynthesis and g_s . We use a factorial suite of
187 model experiments, using the Joint UK land environment simulator (JULES) (Best et al., 2011; Clark et al.,
188 2011), the land-surface model of the UK Earth System Model (UKESM) (Collins et al., 2011) to simulate plant
189 O_3 uptake and damage, and to investigate the impact of both O_3 and CO_2 on plant water-use and carbon uptake.
190 In this work, the JULES model is re-calibrated using the latest observations of vegetation sensitivity to O_3 , with
191 the addition of a separate parameterisation for temperate/boreal regions versus the Mediterranean. The O_3
192 sensitivity of each PFT in JULES was re-calibrated for both a high and low sensitivity to account for uncertainty
193 in the O_3 response, in part due to the observed variation in O_3 sensitivity between species. This includes O_3
194 sensitivities for agricultural crops (wheat – high sensitivity) versus natural grassland (low sensitivity), with
195 separate sensitivities for Mediterranean grasslands. For forests JULES is parameterised with O_3 sensitivities for
196 broadleaf and needle leaf trees (with a high and low O_3 sensitivity for both), with separate sensitivities (high and
197 low) for Mediterranean broadleaf species. We make a separate distinction for the Mediterranean region where
198 possible because the work of Bükér et al. (2015) showed that the sensitivity of dominant Mediterranean trees to
199 O_3 is different to temperate species~~different O_3 dose response relationships are needed to describe the O_3~~
200 ~~sensitivity of dominant Mediterranean trees~~. In addition, we introduce an alternative g_s scheme into JULES as
201 described above. JULES is forced with spatially varying daily O_3 concentrations from a high resolution
202 atmospheric chemistry model for Europe that are disaggregated to hourly concentrations, therefore our
203 simulations account for diurnal variations in O_3 concentration and O_3 responses allowing for improved estimates
204 of O_3 uptake by vegetation. We do not attempt to make a full assessment of the carbon cycle of Europe, instead
205 we target O_3 damage, which is currently a missing component in earlier carbon cycle assessments (Le Quéré et
206 al., 2017; Sitch et al., 2015). To this end, we prescribe changing O_3 and CO_2 concentrations from 1901 to 2050,
207 but use a fixed pre-industrial climate. We acknowledge the use of a 'fixed' pre-industrial climate omits the
208 additional uncertainty of the interaction between climate change and g_s which will affect the rate of O_3 uptake
209 and therefore O_3 concentrations. In addition, using uncoupled chemistry and climate is a further source of
210 uncertainty. To understand the impact of these complex feedback mechanisms is an important area for future
211 work, but in the current study our aim is to isolate the physiological response of plants to both O_3 and CO_2 , and
212 determine the sensitivity of predicted GPP and the land carbon sink to this process, as the impact of O_3 on the
213 land carbon sink currently remains largely unknown at large spatial scales for Europe.

214

215

216

217 **2 Methods**

218

219 **2.1 Representation of O_3 effects in JULES**

220
221
222
223
224
225
226
227
228
229
230
231
232
233
234
235
236
237
238
239
240
241
242
243
244
245
246
247
248
249
250
251
252
253
254
255
256
257
258

JULES calculates the land-atmosphere exchanges of heat, energy, mass, momentum and carbon on a sub-daily time step, and includes a dynamic vegetation model (Best et al., 2011; Clark et al., 2011; Cox, 2001). This work uses JULES version 3.3 (<http://www.jchmr.org>) at 0.5° x 0.5° spatial resolution and hourly model time step, the spatial domain is shown in Fig. S15. JULES has a multi-layer canopy radiation interception and photosynthesis scheme (10 layers in this instance) that accounts for direct and diffuse radiation, sun fleck penetration through the canopy, inhibition of leaf respiration in the light and change in photosynthetic capacity with depth into the canopy (Clark et al., 2011; Mercado et al., 2009). Soil water content also affects the rate of photosynthesis and g_s . It is modelled using a dimensionless soil water stress factor, β , which is related to the mean soil water concentration in the root zone, and the soil water contents at the critical and wilting point (Best *et al.*, 2011).

To simulate the effects of stomatal O₃ deposition on vegetation productivity and water use, JULES uses the flux-gradient approach of Sitch *et al.*, (2007), modified to include non-stomatal deposition following Tuovinen et al. (2009). A similar approach is taken by Franz et al. (2017) in the OCN model, however plant O₃ damage is a function of accumulated O₃ exposure over time. In JULES, plant O₃ damage is instantaneous, because the impact of cumulative O₃ exposure on plant productivity has already been calibrated with observations (described below), the degree to which photosynthesis and g_s are modified at each time step with O₃ exposure having already been calibrated against observations of the change in plant productivity with cumulative O₃ exposure for each PFT (i.e. O₃ dose response functions described later). JULES uses a coupled model of g_s and photosynthesis, the potential net photosynthetic rate (A_p , mol CO₂ m⁻² s⁻¹) is modified by an 'O₃ uptake' factor (F , the fractional reduction in photosynthesis), so that the actual net photosynthesis (A_{net} , mol CO₂ m⁻² s⁻¹) is given by equation 1 (Clark *et al.*, 2011, Sitch *et al.*, 2007). Because of the relationship between these two fluxes, the direct effect of O₃ damage on photosynthetic rate also leads to a reduction in g_s . An alternative approach was taken by Lombardozzi et al. (2012) in the CLM model where photosynthesis and g_s are decoupled, so that O₃ exposure affects carbon assimilation and transpiration independently. In JULES, changes in atmospheric CO₂ concentration also affect photosynthetic rate and g_s , consequently the interaction between interactive effects of changing concentrations of both CO₂ and O₃ is allowed for.

$$A_{net} = A_p F \tag{1}$$

The O₃ uptake factor (F) is defined as:

$$F = 1 - a * \max[F_{O_3} - F_{O_3crit}, 0.0] \tag{2}$$

F_{O_3} is the instantaneous leaf uptake of O₃ (nmol m⁻² s⁻¹), F_{O_3crit} is a PFT-specific threshold for O₃ damage (nmol m⁻² PLA s⁻¹, projected leaf area), and 'a' is a PFT-specific parameter representing the fractional reduction of photosynthesis with O₃ uptake by leaves. Following Tuovinen et al. (2009), the flux of O₃ through stomata, F_{O_3} , is represented as follows:

259
$$F_{O_3} = O_3 \left(\frac{g_b \left(\frac{g_l}{K_{O_3}} \right)}{g_b + \left(\frac{g_l}{K_{O_3}} \right) + g_{ext}} \right)$$
 (3a)

260

261 O_3 is the molar concentration of O_3 at reference (canopy) level (nmol m^{-3}), g_b is the leaf-scale boundary layer
 262 conductance (m s^{-1} , eq 3b), g_l is the leaf conductance for water (m s^{-1}), K_{O_3} accounts for the different diffusivity of
 263 ozone to water vapour and takes a value of 1.51 after Massman (1998), and g_{ext} is the leaf-scale non-stomatal
 264 deposition to external plant surfaces (m s^{-1}) which takes a constant value of 0.0004 m s^{-1} after Tuovinen et al.
 265 (2009). The leaf-level boundary layer conductance (g_b) is calculated as in Tuovinen *et al.* (2009)

266

267
$$g_b = \alpha L d^{-1/2} U^{-1/2}$$
 (3b)

268

269 α is a constant ($0.0051 \text{ m s}^{-1/2}$), Ld is the cross-wind leaf dimension (m) defined per PFT as 0.05 for trees, 0.02
 270 for grasses (C_3 and C_4) and 0.04 for shrubs, U is wind speed at canopy height (m s^{-1}). The rate of O_3 uptake is
 271 dependent on g_s , which is dependent on photosynthetic rate. Given g_s is a linear function of photosynthetic rate in
 272 JULES (Clark et al., 2011), from eq 1 it follows that:

273

274
$$g_s = g_l F$$
 (4)

275

276 The O_3 flux to stomata, F_{O_3} , is calculated at leaf level and then scaled to each canopy layer differentiating sunlit
 277 and shaded leaf photosynthesis, and finally summed up to the canopy level. Because the photosynthetic capacity,
 278 photosynthesis and therefore g_s decline with depth into the canopy, this in turn affects O_3 uptake, with the top leaf
 279 level contributing most to the total O_3 flux and the lowest level contributing least.

280

281 2.2 Calibration of O_3 uptake model

282

283 Here we use the latest literature on flux based O_3 dose-response relationships derived from observed field data
 284 across Europe (CLRTAP, 2017) to determine the key PFT-specific O_3 sensitivity parameters in JULES (a and
 285 F_{O_3crit}). Synthesis of information expressed as O_3 flux based dose-response relationships derived from field
 286 experiments is carried out by The United Nations Convention on Long-Range Transboundary Air Pollution
 287 (CLRTAP Convention), this information is then used as a policy tool to inform emission reduction strategies in
 288 Europe to improve air quality (CLRTAP, 2017; Mills et al., 2011a). Derivation of O_3 flux based dose-response
 289 relationships for different vegetation types uses the accumulated stomatal O_3 flux above a threshold (often referred
 290 to as the phytotoxic O_3 dose above a threshold of ‘y’ i.e. POD_y) as the dose metric, and the percentage change in
 291 biomass as the response metric (Emberson et al., 2007; Karlsson et al., 2007). We use these observation based O_3
 292 dose-response relationships to calibrate each JULES PFT for sensitivity to O_3 using available relationships for the
 293 closest matching vegetation type. For JULES, F_{O_3crit} is the threshold for O_3 damage, and values for this parameter
 294 are taken from the O_3 dose-response relationships as the POD_y value (see CLRTAP, 2017 and Buker et al. 2015
 295 for derivation of POD_y values). The actual sensitivity to O_3 is determined by the slope of the O_3 dose-response
 296 relationship, i.e. how much biomass changes with accumulated stomatal uptake of O_3 above the damage threshold,
 297 this relates to the parameter a in JULES. The parameter ‘ a ’ is a PFT-specific parameter representing the fractional

298 reduction of photosynthesis with O₃ uptake by leaves. Values for this parameter are found for each PFT by running
299 JULES with different values of 'a', which alter the instantaneous photosynthetic rate, but then calculating the
300 accumulated stomatal flux of O₃ and the change in productivity, until the slope of this relationship produced by
301 the JULES simulations matches that of the O₃ dose-response relationships derived from observations. Essentially
302 we calibrate each JULES PFT for sensitivity to O₃ by reproducing the observation-based O₃ dose-response
303 relationships.

304

305 Each PFT was calibrated for ~~a~~ high and low plant O₃ sensitivity to account for uncertainty in the sensitivity of
306 different plant species to O₃, using the approach of Sitch *et al.*, (2007). Therefore, when using our results to assess
307 the impact of O₃ at the land surface, we are able to provide a range in our estimates to help address some of the
308 uncertainty in the O₃ response of different vegetation types. In addition, where possible owing to available data,
309 a distinction was made for Mediterranean regions. This was because the work of Bükér *et al.* (2015) showed that
310 different O₃ dose-response relationships are needed to describe the O₃ sensitivity of dominant Mediterranean trees.
311 For the C₃ herbaceous PFT, the dominant land cover type across the European domain in this study (Fig. S24),
312 the high plant O₃ sensitivity was calibrated against observations for wheat to give a representation of agricultural
313 regions and wheat is one of the most sensitive grasses to O₃ (Fig. S32, Table S1). For the low plant O₃ sensitivity
314 JULES was calibrated against the dose-response function for natural grassland to give a representation of natural
315 grassland and this vegetation has a much lower sensitivity to O₃ damage, for the Mediterranean region we used a
316 function for Mediterranean natural grasslands, all taken from CLRTAP (2017) (Fig. S32, Table S1). Tree/shrub
317 PFTs were calibrated against observed O₃ dose-response functions for the high plant O₃ sensitivity: broadleaf
318 trees (temperate/boreal) = Birch/Beech dose-response relationship, broadleaf trees (Mediterranean) = deciduous
319 oaks dose-response relationship, needle leaf trees = Norway spruce dose-response relationship, shrubs =
320 Birch/Beech dose-response relationship, all from CLRTAP (2017) (Fig. S32, Table S1). Data on O₃ dose-response
321 relationships for different vegetation types is very limited, therefore for the low plant O₃ sensitivity calibration for
322 trees/shrubs we assumed a 20% decrease in sensitivity to O₃ based on the difference in sensitivity between high
323 and low sensitive tree species in the Karlsson *et al.* (2007) study. Due to limitations in data availability, the shrub
324 parameterisation uses the observed dose-response functions for broadleaf trees. Similarly, the parameterisation
325 for C₄ herbaceous uses the observed dose-responses for C₃ herbaceous, however the fractional cover of C₄ herbs
326 across Europe is low (Fig. S24), so this assumption affects a very small percentage of land cover.

327

328 To calibrate the JULES O₃ uptake model, JULES was run across Europe forced using the WFDEI observational
329 climate dataset (Weedon, 2013) at 0.5° X 0.5° spatial and three hour temporal resolution. JULES uses interpolation
330 to disaggregate the forcing data down from 3 hours to an hourly model time step. The model was spun-up over
331 the period 1979 to 1999 with a fixed atmospheric CO₂ concentration of 368.33 ppm (1999 value from Mauna Loa
332 observations (Tans and Keeling, 2014), ~~(Tans and Keeling)~~). Zero tropospheric ozone concentration was assumed
333 for the control simulation, for the simulations with O₃, spin-up used spatially explicit fields of present day O₃
334 concentration produced using the UK Chemistry and Aerosol (UKCA) model with standard chemistry from the
335 run evaluated by O'Connor *et al.* (2014). A fixed land cover map was used based on IGBP (International
336 Geosphere-Biosphere Programme) land cover classes (IGBP-DIS), therefore as the vegetation distribution was
337 fixed and the calibration was not looking at carbon stores, a short spin-up was adequate to equilibrate soil

338 temperature and soil moisture. JULES was then run for the year 2000 with a corresponding CO₂ concentration of
 339 369.52 ppm (from Mauna Loa observations (Tans and Keeling, 2014), ~~(Tans and Keeling)~~) and monthly fields of
 340 spatially explicit tropospheric O₃ (O'Connor et al., 2014) as necessary.

341

342 Calibration was performed using four simulations: with i) zero tropospheric O₃ concentration, this was the control
 343 simulation (control), ii) tropospheric O₃ at current ambient concentration (O3), iii) ambient +20 ppb (O3+20) and
 344 iv) ambient +40 ppb (O3+40). The different O₃ simulations (i.e. O3, O3+20 and O3+40) were used to capture the
 345 range of O₃ conditions in the data used in the observation-based O₃ dose-response relationships used in this study
 346 for calibration, often data were from experiments using artificially manipulated conditions of ambient + 40 ppb
 347 O₃ for example. For each JULES O₃ simulation, the value of F_{O_3crit} was taken from the vegetation specific O₃
 348 dose-response relationship as the threshold O₃ concentration above which damage to vegetation occurs. An initial
 349 estimate of the parameter 'a' was used, then for each PFT and each simulation, hourly estimates of NPP (our
 350 proxy for biomass – although not identical they are related) and O₃ uptake in excess of F_{O_3crit} were accumulated
 351 over a PFT dependent accumulation period. The accumulation periods were ~6 months for broadleaf trees and
 352 shrubs, all year for needle leaf trees, and ~3 months for herbaceous species, through the growing season, following
 353 guidelines in CLRTAP (2017). Additionally, in accordance with the methods used in the CLRTAP (2017) that
 354 describe how the O₃ dose-response relationships are derived from observations, we use the stomatal O₃ flux per
 355 projected leaf area to top canopy sunlit leaves. The percentage change in total NPP was calculated for each O₃
 356 simulation and plotted against the cumulative uptake of O₃ over the PFT-specific accumulation period. The linear
 357 regression of this relationship was calculated, and slope and intercept compared against the slope and intercept of
 358 the observed dose-response relationships. Values of the parameter 'a' were adjusted, and the procedure repeated
 359 until the linear regression through the simulation points matched that of the observations (Fig. S32, Table S1).

360

361 **2.3 Representation of stomatal conductance and site level evaluation**

362

363 In JULES, g_s (m s⁻¹) is represented following the closure proposed by (Jacobs, 1994):

364

$$365 \quad g_s = 1.6RT_l \frac{A_{net}\beta}{c_a - c_i} \quad (5)$$

366

367 In this parameterisation, c_i is unknown and in the default JULES model is calculated as in equation 6, hereafter
 368 called JAC:

369

$$370 \quad c_i = (c_a - c_*)f_0 \left(1 - \frac{dq}{dq_{crit}}\right) + c_* \quad (6)$$

371

372 β is a soil moisture stress factor, the factor 1.6 accounts for g_s being the conductance for water vapour rather than
 373 CO₂, R is the universal gas constant (J K⁻¹ mol⁻¹), T_l is the leaf surface temperature (K), c_a and c_i (both Pa) are the
 374 leaf surface and internal CO₂ partial pressures, respectively, c_* (Pa) is the CO₂ photorespiration compensation
 375 point, dq is the humidity deficit at the leaf surface (kg kg⁻¹), dq_{crit} (kg kg⁻¹) and f_0 are PFT specific parameters

376 representing the critical humidity deficit at the leaf surface, and the leaf internal to atmospheric CO₂ ratio (c_i/c_a)
377 at the leaf specific humidity deficit (Best *et al.* 2011), values are shown in Table S1.

378

379 In this work, we replace equation 6 with the closure described in Medlyn *et al.* (2011), using the key PFT specific
380 model parameter g_l (kPa^{0.5}), and dq is expressed in kPa, shown in eq 7, hereafter called MED:

381

$$382 \quad c_i = c_a \left(\frac{g_l}{g_l + \sqrt{dq}} \right) \quad (7)$$

383

384 PFT specific values of the g_l parameter were derived for European vegetation from the data base of Lin *et al.*
385 (2015) and are shown in Table S1. The g_l parameter represents the sensitivity of g_s to the assimilation rate, i.e.
386 plant water use efficiency, and was derived as in Lin *et al.* (2015) by fitting the Medlyn *et al.*, (2011) model to
387 observations of g_s , photosynthesis, and VPD, assuming an intercept of zero-with no g_l term.

388

389 The impact of g_s model formulation (JAC versus MED) on simulated water, O₃, carbon and energy fluxes is
390 compared for two contrasting grid points - wet (low soil moisture stress) and dry (high soil moisture stress) in the
391 European domain. JULES was spun-up for 20 years (1979-1999) at two grid points in central Europe representing
392 a wet (low soil moisture stress, lat: 48.25; lon.: 5.25) and a dry site (high soil moisture stress, lat: 38.25; lon.: -
393 7.75). The modelled soil moisture stress factor ($fsmc$) at the wet site ranged from 0.8 to 1.0 over the year 2000
394 (1.0 indicates no soil moisture stress), and at the dry site $fsmc$ steadily declined from 0.8 at the start of the year to
395 0.25 by the end of the summer. The WFDEI meteorological forcing dataset was used (Weedon, 2013), along with
396 atmospheric CO₂ concentration for the year 1999 (368.33 ppm), and either no O₃ (i.e. the O₃ damage model was
397 switched off) for the control simulations, or spatially explicit fields of present day O₃ concentration produced
398 using the UK Chemistry and Aerosol (UKCA) model from the run evaluated by O'Connor *et al.* (2014) for the
399 simulations with O₃. Following the spin-up period, JULES was run for one year (2000) with corresponding
400 atmospheric CO₂ concentration, and tropospheric O₃ concentrations as described above. The control and O₃
401 simulations were performed for both JAC and MED model formulations. Land cover for the spin-up and main run
402 was fixed at 20% for each PFT. For the simulations including O₃ damage, the high plant O₃ sensitivity
403 parameterisation was used. The difference between these simulations was used to assess the impact of g_s model
404 formulation on the leaf level fluxes of carbon and water. We calculate and report (results section 3.1) the difference
405 in mean annual water-use that results from the above simulations using the different g_s models. For each day of
406 the simulation we calculate the percentage difference in water-use between the two simulations, we then calculate
407 the mean and standard deviation over the year to give the annual mean leaf-level water-use.

408

409 Site level evaluation of the two g_s models compared to FLUXNET observations was carried out to evaluate the
410 seasonal cycles of latent and sensible heat using the two g_s models JAC and MED compared to observations.
411 Seven Fluxnet towers were selected to represent a range of land cover types as shown in Table S2. JULES was
412 setup for each site using observed site-level hourly meteorology, and the vegetation cover was prescribed
413 according to the fractional covers of the different JULES surface types shown in Table S2. Following a spin-up
414 period, simulations were run at each site for the years shown in Table S2.

415

416 2.4 Model simulations for Europe

417

418 2.4.1 Forcing datasets

419

420 We used the WATCH meteorological forcing data set (Weedon et al., 2010; Weedon et al., 2011) at 0.5° x 0.5°
421 spatial and three hour temporal resolution for our JULES simulations. JULES interpolates this down to an hourly
422 model time step. For this study, the climate was kept constant by recycling over the period 1901 to 1920, to allow
423 us to focus on the impact of O₃, CO₂ and their interactive effects.

424

425 JULES was run with prescribed annual mean atmospheric CO₂ concentrations. Pre-industrial global CO₂
426 concentrations (1900 to 1960) were taken from Etheridge et al. (1996), 1960 to 2002 were from Mauna Loa
427 (Keeling and Whorf, 2004), as calculated by the Global Carbon Project (Le Quéré et al., 2016), and 2003-2050
428 were based on the IPCC SRES A1B scenario and were linearly interpolated to gap fill missing years (Fig. 1).

429

430 JULES was run including dynamic vegetation with a land cover mask giving the fraction of agriculture in each
431 0.5° x 0.5° grid cell based on the Hurtt et al. (2011) land cover database for the year 2000. The agricultural mask
432 is fixed and does not change over the simulation period. This means that whilst the model is allowed to evolve its
433 own vegetation cover outside of the agricultural mask, within the ~~agricultural~~ mask only C₃/C₄ herbaceous PFTs
434 are allowed to grow, with no competition from other PFTs. Therefore, through the simulation period, regions of
435 agriculture are maintained as such and not out-competed by forests for example, allowing for a more accurate
436 representation of the land cover of Europe in the model. No form of land management is simulated (i.e. no crop
437 harvesting, ploughing, rotation or grazing), growth and leaf area index (LAI) are determined by resource
438 availability and phenology. Outside of the agricultural mask, dynamic vegetation means that grid cell PFT
439 coverage and LAI are the result of resource availability, phenology and simulated competition. Across the model
440 domain, simulated mean annual LAI was dominantly within the range of 2 to 5 m²/m² (Fig. S43 and S54).
441 Following a full spin-up period (to ensure equilibrium vegetation, carbon and water states), there was no
442 significant change in the fractional cover of each PFT over the simulation period (1901 - 2050). By 2050, increases
443 in boreal forest cover occurred, but this was less than 2% and limited to very small areas, given this small change
444 we show just the land cover for 2050 in Fig. S21.

445

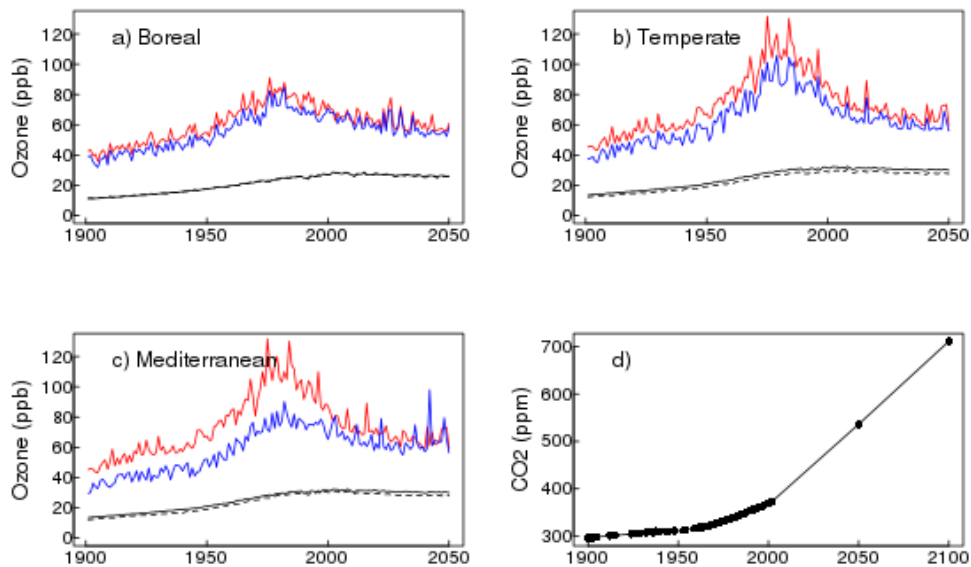
446 Tropospheric O₃ concentration was produced by the EMEP MSC-W model at 0.5° x 0.5° (Simpson et al., 2012),
447 driven with meteorology from the regional climate model RCA3 (Kjellström et al., 2011; Samuelsson et al., 2011),
448 which provides a downscaling of the ECHAM A1B-r3 (simulation 11 of Kjellström et al., 2011). This setup
449 (EMEP+RCA3) is also used by Langner et al. (2012a), Simpson et al. (2014a), Tuovinen et al. (2013), Franz et
450 al. (2017) and Engardt et al. (2017), where further details and model evaluation can be found. Unfortunately, the
451 3-dimensional RCA3 data needed by the EMEP model was not available prior to 1960, but as in Engardt et al.
452 (2017) the meteorology of 1900-1959 had to be approximated by assigning random years from 1960 to 1969. This
453 procedure introduces some uncertainty of course, although Langner et al. (2012b) show that for the period 1990
454 to 2100 it is emissions change, rather than meteorological change, that drives modelled O₃ concentrations. The

455 emissions scenarios for 1900-2050 merge data from the International Institute of Applied System Analysis
456 (IIASA) for 2005-2050 (the so-called ECLIPSE 4a scenario), recently revised EMEP data for 1990, and a scaling
457 back from 1990 to 1900 using data from Lamarque et al. (2013). The trend in emissions of the major O₃ precursors
458 NO_x, NMVOC and Isoprene are shown from 1900 to 2050 over Europe in Fig. S65. Isoprene emissions are not
459 inputs to the EMEP model, but rather calculated at each time-step using temperature, radiation, and land-cover
460 specific emission factors (Simpson et al., 2012). Changes in the assumed background concentration of CH₄ (from
461 RCP6.0) (van Vuuren et al., 2011) are also shown in Fig. S65. Engardt et al. (2017) show the trend in emissions
462 of SO₂ and NH₃ from 1900 to 2050 over Europe. The EMEP model accounts for changes in BVOC emissions as
463 a result of predicted ambient temperature changes.

464
465 O₃ concentrations from EMEP MSC-W were calculated at canopy height for two land-cover categories: forest
466 and grassland (Fig. S76 and Fig. S87), which are taken as surrogates for high and low vegetation, respectively.
467 These canopy-height specific concentrations allow for the large gradients in O₃ concentration that can occur in
468 the lowest 10s of metres, giving lower O₃ for grasslands than seen at e.g. 20 m in a forest canopy (Gerosa et al.,
469 2017; Simpson et al., 2012; Tuovinen et al., 2009). These canopy level O₃ concentrations are used as input to
470 JULES, using the EMEP O₃ concentrations for forest for the forest JULES PFTs (broadleaf/needle leaf tree and
471 shrub), and the EMEP O₃ concentrations for grassland for the grass/herbaceous JULES PFTs (C₃ and C₄). This
472 study used daily mean values of tropospheric O₃ concentration from EMEP disaggregated down to the hourly
473 JULES model time-step. The daily mean O₃ forcing was disaggregated to follow a mean diurnal profile of O₃, this
474 was generated from hourly O₃ output from EMEP MSC-W for the two land cover categories (forest and grassland
475 as described above) across the same model domain. O₃ concentrations follow a diurnal cycle and peak during the
476 day, therefore accounting for the diurnal variation in O₃ concentrations allows for a more realistic estimation of
477 O₃ uptake.

478
479 Figure 1 shows large increases in tropospheric O₃ from pre-industrial to present day (2001), this is in line with
480 modelling studies (Young et al., 2013) and site observations (Derwent et al., 2008; Logan et al., 2012; Parrish et
481 al., 2012), and is predominantly a result of increasing anthropogenic emissions (Young et al., 2013). Figures S76
482 and S87 show this large increase in ground-level O₃ concentrations from 1901 to 2001 occurs in all seasons.
483 Present day O₃ concentration show a strong seasonal cycle, with a spring/summer peak in concentrations in the
484 mid-latitudes of the Northern Hemisphere (Derwent et al., 2008; Parrish et al., 2012; Vingarzan, 2004). Seasonal
485 cycles have been changing over the past decades however, attributed to changes in NO_x and other emissions, as
486 well as changes in transport patterns (Parrish et al., 2013). These changes will likely continue in future as
487 emissions and meteorological factors impact photo-chemical O₃ production and transport patterns. Indeed, the O₃
488 concentrations used in the simulations in this study show increased O₃ levels in winter and in some regions in
489 autumn and spring in 2050 compared to present day, this may be due to reduced titration of O₃ by NO as a result
490 of reduced NO_x emissions in the future (Royal Society, 2008). Summer O₃ concentrations are lower in 2050
491 however, compared to 2001.

492
493



494

495 **Figure 1.** Regional time series of canopy height O₃ (ppb) forcing from EMEP a) to c), and d) global atmospheric
 496 CO₂ (ppm) concentration (this does not vary regionally; black dots show data points, the black line shows
 497 interpolated points). Each panel for the O₃ forcing shows the regional annual average (woody PFTs, black solid
 498 line; herbaceous PFTs, black dashed line) and the annual maximum O₃ concentration above: woody PFTs (red)
 499 and herbaceous PFTs (blue).

500

501 2.4.2 Spin up and factorial experiments

502

503 JULES was spun-up by recycling the climate from the early part of the twentieth century (1901 to 1920) using
 504 atmospheric CO₂ (296.1 ppm) and O₃ concentrations from 1901 (Fig. S73 & Fig. S84). Model spin-up was 2000
 505 years by which point the carbon pools and fluxes were in steady state with zero mean net land – atmosphere CO₂
 506 flux. We performed the following transient simulations for the period 1901 to 2050 with continued recycling of
 507 the climate as used in the spin-up, for both high and low plant O₃ sensitivities:

508

- 509 • **run_O3** : Fixed 1901 CO₂, Varying O₃
- 510 • **run_CO2** : Varying CO₂, Fixed 1901 O₃
- 511 • **run_both_CO2+O3** : Varying CO₂, Varying O₃

512

513 We use these simulations to investigate the direct effects of changing atmospheric CO₂ and O₃ concentrations,
 514 individually and combined, on plant water-use, GPP and the land C sink through the twentieth century and into
 515 the future, specifically over three time periods: historical (1901-2001), future (2001-2050) and over the full time
 516 series (1901-2050). For each time period we calculate the difference between the decadal means calculated at the
 517 start and end of the analysis period for each variable of interest. Therefore our results report the change in GPP,
 518 for example, over the analysis period. For each variable analysed (GPP, NPP, vegetation carbon, soil carbon, total
 519 land carbon and *g_s*), we use the mean over 10 years to represent each time period, e.g. the mean over 2040 to 2050
 520 is what we call 2050, 1901 to 1910 is what we refer to as 1901. The difference between the simulations gives the
 521 effect of O₃ and CO₂ either separately or in combination over the different time periods. We look at the percentage

522 change due to either O₃ at pre-industrial CO₂ concentration (i.e. without the additional effect of atmospheric CO₂
 523 on stomatal behaviour ~~run O₃ simulation~~), CO₂ (at fixed pre-industrial O₃ concentration, ~~run CO₂ simulation~~)
 524 or the combined effect of both gases (~~run both CO₂+O₃ simulation~~), e.g. $100 * (\text{varO}_3[2050] - \text{varO}_3[1901]) /$
 525 $\text{varO}_3[1901]$ gives the O₃ effect (at fixed CO₂) over the full experimental period. The meteorological forcing is
 526 prescribed in these simulations and is therefore the same between the model runs. Other climate factors, such as
 527 VPD, temperature and soil moisture availability are accounted for in our simulations, but our analysis isolates the
 528 effects of O₃, CO₂ and O₃ + CO₂. We also use paired t-test to determine statistically significant differences between
 529 the different (high and low) plant O₃ sensitivities.

530 ~~which is calculated as:~~

531 ~~$100 * (\text{var}[y_1] - \text{var}[y_2]) / \text{var}[y_2]$~~ ~~(~~

532 ~~Where var[y_x] represents the variable in time period y,~~

533 2.4.3 Evaluation

534 To evaluate our JULES simulations we compare mean GPP from 1991 to 2001 for each of the JULES scenarios
 535 and both high and low plant O₃ sensitivities against the observation based globally extrapolated Flux Network
 536 model tree ensemble (MTE) (Jung et al., 2011). We use paired t-test to determine statistically significant
 537 differences in the mean responses.

538

539 3 Results

540

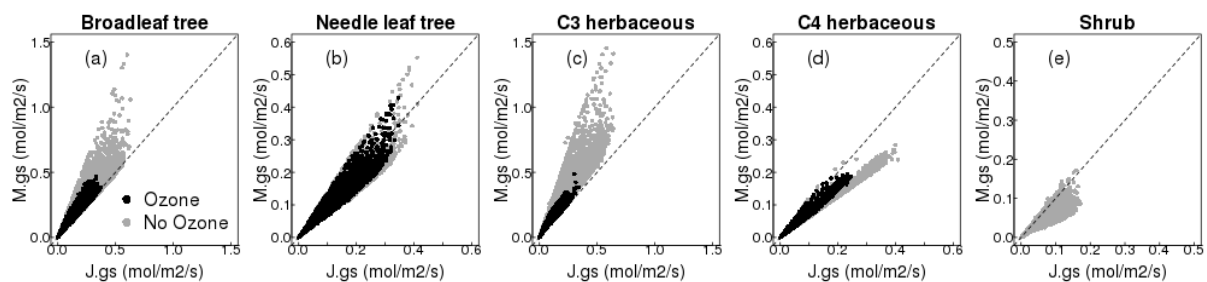
541 3.1 Impact of g_s model formulation and site level evaluation

542

543 The impact of g_s model on simulated g_s is shown for the site with low soil moisture stress (wet site, Fig. 2). For
 544 the broadleaf tree and C₃ herbaceous PFT, the MED model simulates a larger conductance compared to the JAC
 545 model. In other words, with the MED model these two PFTs are parameterised with a less conservative water use
 546 strategy, which, for the grid point shown in Fig. 2, increased the annual mean water use by 35% (±29%) and 45%
 547 (±32%), respectively. In contrast, the needle leaf tree, C₄ herbaceous and shrub PFTs are parameterised with a
 548 more conservative water use strategy with the MED model, and the mean annual g_s was decreased by 13% (±12%),
 549 27% (±10%) and 36% (±13%), respectively, compared to the JAC model. This comparison was also done for a
 550 dry site (high soil moisture stress), and similar results were found (Fig. S98). The effect of g_s formulation on
 551 simulated photosynthesis was much smaller because of the lower sensitivity of the limiting rates of photosynthesis
 552 to changes in c_i in the model compared to the effect of the same change in c_i on modelled g_s (Fig. S109 & S1140).
 553 Changes in g_s impact the partitioning of simulated energy fluxes. In general, increased g_s results in increased latent
 554 heat and thus decreased sensible heat flux, and vice versa where g_s is decreased (Fig. S109 & S1140). Also shown
 555 is the effect of the MED model on O₃ flux into the leaf (Fig. S1244 and Fig. S98 bottom panel). For the broadleaf
 556 tree and C₃ herbaceous PFT, the MED model simulates a larger conductance and therefore a greater flux of O₃
 557 through stomata compared to JAC, and this is indicative of the potential for greater reductions in photosynthesis
 558 (Fig. S109 & S1140 top row). The reverse is seen for the needle leaf tree, C₄ herbaceous and shrub PFTs.

559

560 Site level evaluation of the seasonal cycles of latent and sensible heat with both JAC and MED models compared
 561 to FLUXNET observations showed in general, the MED model improved the seasonal cycle of both fluxes (lower
 562 RMSE), but the magnitude of this varied from site to site (Fig. S13+2). At the deciduous broadleaf site, US-UMB,
 563 MED resulted in improvements of the simulated seasonal cycle particularly in the summer months for both fluxes
 564 (RMSE decreased from 42.7/31.5 to 38.5/28.0 W/m² for latent/sensible heat respectively). At the second
 565 deciduous broadleaf site IT-CA1 however, there was almost no difference between the two g_s models. Both
 566 evergreen needle leaf forest sites (FI-Hyy and DE-Tha) saw improvements in the simulated seasonal cycles of
 567 latent and sensible heat with the MED model, primarily as a result of lower latent heat flux in the spring and
 568 summer months, and higher sensible heat flux over the same period. At FI-Hyy, RMSE decreased from 10.1/7.4
 569 to 6.7/6.7 W/m² for latent/sensible heat respectively, and at DE-Tha, RMSE decreased from 16.0/11.9 to 10.5/10.6
 570 W/m² for latent/sensible heat respectively. With the MED model the monthly mean latent heat flux was improved
 571 at the C₃ grass site (CH-Cha) as a result of increased flux in the summer months (RMSE decreased from 15.7 to
 572 13.8 W/m²), however there was no improvement in the sensible heat flux and RMSE with MED was increased
 573 (from 3.9 to 4.9 W/m²). At the C₄ grass site (US-SRG), small improvements were made in the seasonal cycle of
 574 both latent and sensible heat with the MED model. At the deciduous savannah site (CG-Tch) which included a
 575 high proportion of shrub PFT in the land cover type used in the site simulation, large improvements in the seasonal
 576 cycle of both fluxes were simulated with the MED model, as a result of a decrease in the latent heat flux and an
 577 increase in the sensible heat flux (RMSE decreased from 39.5/31.6 to 30.4/24.4 W/m² for latent/sensible heat
 578 respectively).



579

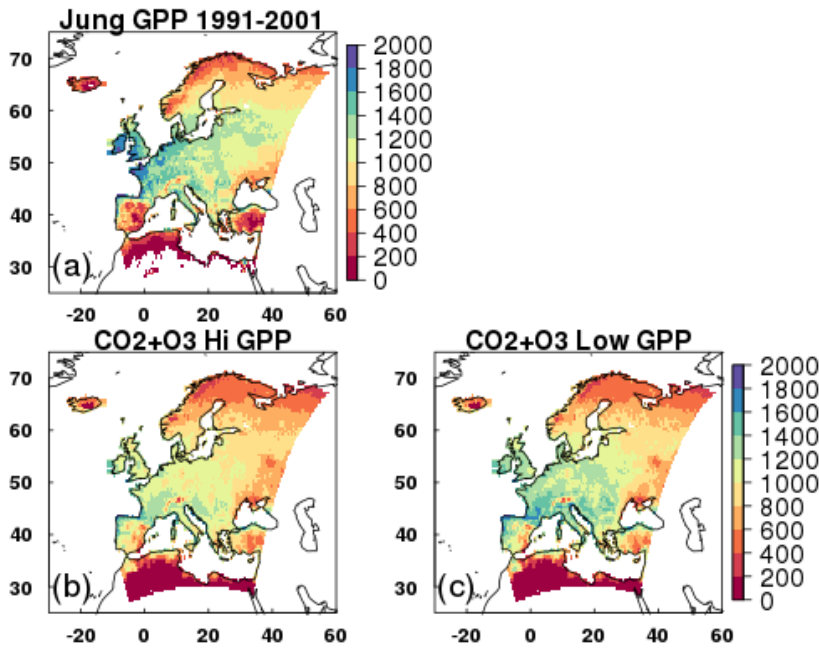
580 **Figure 2.** Comparison of simulated g_s with MED (y axis) versus JAC (x axis) for all five JULES PFTs at one grid
 581 point (lat: 48.25; lon: 5.25) shown are hourly values for the year 2000 (see SI section S3 for further details).

582

583 3.2 Evaluation of the JULES O₃ model

584 For all JULES scenarios similar spatial patterns of GPP are simulated compared to MTE (Fig. 3 and Fig. S14+3).
 585 MTE estimates a mean GPP for present day in Europe of 938 gC m² yr⁻¹ (Fig. 3). JULES tends to under-predict
 586 GPP relative to the MTE product, estimates of GPP from JULES with both transient CO₂ and O₃
 587 (run_both CO₂+O₃-simulation) gives a mean across Europe of 813 gC m² yr⁻¹ (high plant O₃ sensitivity) to 881
 588 gC m² yr⁻¹ (low plant O₃ sensitivity), both of which are significantly different to the MTE product ($t=27$, $d.f.=5750$,
 589 $p<2.2e^{-16}$ (high); $t=4.3$, $d.f.=5750$, $p<1.5e^{-05}$ (low); Fig. 3). Forcing with CO₂ alone (run_CO2-simulation) gives a
 590 mean GPP across Europe of 900 to 923 gC m² yr⁻¹ (high and low plant O₃ sensitivity respectively), and O₃ alone
 591 (run_O3-simulation - without the protective effect of CO₂) reduces estimated GPP to 732 to 799 gC m² yr⁻¹ (Fig.

592 [S1413](#)). At latitudes $>45^{\circ}\text{N}$ JULES has a tendency to under-predict MTE-GPP, and at latitudes $<45^{\circ}\text{N}$ JULES
 593 tends to over-predict MTE-GPP (Fig. [S1514](#)). These regional differences are highlighted in Fig. [S1615](#), where in
 594 the Mediterranean region, JULES tends to over-predict compared to MTE-GPP, so simulations with O_3 reduce
 595 the simulated GPP bringing it closer to MTE. In the temperate region however, JULES tends to under-estimate
 596 MTE-GPP, so the addition of O_3 reduces simulated GPP further (Fig. [S1615](#)). In the boreal region, JULES under-
 597 predicts GPP, but to a lesser extent than in the temperate region, and the addition of O_3 has less impact on reducing
 598 the GPP further (Fig. [S1615](#)).
 599



600
 601 **Figure 3.** Mean GPP ($\text{g C m}^2 \text{ yr}^{-1}$) from 1991 to 2001 for a) the observationally based globally extrapolated Flux
 602 Network model tree ensemble (MTE) (*Jung et al.*, 2011); b, c) model simulations with transient CO_2 and transient
 603 O_3 ([run_both_CO2+O3](#)), high and low plant O_3 sensitivity respectively.
 604

605
 606 **3.3 European simulations - Historical Period: 1901-2001**
 607

608 Over the historical period (1901-2001), [run_O3-\(O3-simulation\)](#) reduced GPP under both the low and high plant
 609 O_3 sensitivity parameterizations by -3% to -9% respectively (Table 1), and this difference in simulated GPP was
 610 significant ($t=102.2$, $d.f.=6270$, $p<2.2e^{-16}$). Figure 4 highlights regional variations, however, where simulated
 611 reductions in GPP are up to 20% across large areas of Europe, and up to 30% in some Mediterranean regions
 612 under the high plant O_3 sensitivity. Some Boreal and Mediterranean regions show small increases in GPP over
 613 this period, associated with O_3 induced stomatal closure enhancing water availability in these drier regions (Fig.
 614 5). This allows for greater stomatal conductance later in the year when soil moisture may otherwise have been
 615 limiting to growth (up to 10%, Fig. 5), and therefore higher GPP, but these regions comprise only a small area of

616 the entire domain. Indeed, over much of the Europe, O₃-induced stomatal closure led to reduced g_s (up to 20%)
617 across large areas of temperate Europe and the Mediterranean, and even greater reductions in some smaller regions
618 of southern Mediterranean (Fig. 6), and these are not associated with notable increases in soil moisture availability
619 (Fig. 5), resulting in depressed GPP over much of Europe as described above. Under the low plant O₃ sensitivity,
620 similar spatial patterns occur, but the magnitude of GPP change (up to -10% across much of Europe) and g_s change
621 (-5% to -10%) are lower compared to the high sensitivity. Over the twentieth century the land carbon sink is
622 suppressed (-2% to -6%, Table 1). Large regional variation is shown in Figure 4, with temperate and
623 Mediterranean Europe seeing a large reduction in land carbon storage, particularly under the high plant O₃
624 sensitivity (up to -15%).

625

626 Combined, the physiological response to changing CO₂ and O₃ concentrations (run_both_CO2+O3-simulation)
627 results in a net loss of land carbon over the twentieth century under the high plant O₃ sensitivity (-2%, Table 1),
628 dominated by loss of soil carbon (Table S3). This reflects the large increases in tropospheric O₃ concentration
629 observed over this period (Fig. 1). Under the low plant O₃ sensitivity, the land carbon sink has started to recover
630 by 2001 (+1.5%) owing to the recovery of the soil carbon pool beyond 1901 values over this period (Table S3).

631

632 To gain perspective on the magnitude of the O₃ induced flux of carbon from the land to the atmosphere we relate
633 changes in total land carbon to carbon emissions from fossil fuel combustion and cement production for the EU-
634 28-plus countries from the data of Boden et al. (2013). We recognise that our simulation domain is slightly larger
635 than the EU28-plus as it includes a small area of western Russia so direct comparisons cannot be made, but this
636 still provides a useful measure of the size of the carbon flux. For the period 1970 to 1979 the simulated loss of
637 carbon from the European terrestrial biosphere due to O₃ effects on vegetation physiology was on average 1.32
638 Pg C (high vegetation sensitivity) and 0.71 Pg C (low vegetation sensitivity) (Table 2). This O₃ induced reduced
639 C uptake of the land surface is equivalent to around 8% to 16% of the emissions of carbon from fossil fuel
640 combustion and cement production over the same period for the EU28-plus countries (Table 2). Currently the
641 emissions data availability goes up to 2011, over the last observable decade (2002 to 2011) the simulated reduction
642 in land carbon due to O₃ has declined, but is still equivalent to 2% to 4% of the emissions of carbon from fossil
643 fuels and cement production for the EU28-plus countries (Table 2). By comparison with one of the largest
644 anthropogenic emissions of carbon for Europe, we show here the potential effect of O₃ on reducing the size of the
645 European land carbon sink is notable.

646

647 **3.4 European simulations - Future Period: 2001-2050**

648

649 Over the 2001 to 2050 period, region-wide GPP with O₃ only changing (run_O3-simulation) increased marginally
650 (+0.1% to +0.2%, high and low plant O₃ sensitivity, Table 1, with a significant difference between the two plant
651 O₃ sensitivities ($t=57, d.f.=6270, p<2.2e^{-16}$)), although with large spatial variability as discussed below (Fig. 4g &
652 h). Figures S76 and S87 show that despite decreased tropospheric O₃ concentrations by 2050 in summer compared
653 to 2001 levels, all regions are exposed to an increase in O₃ over the wintertime, and some regions of Europe,
654 particularly temperate/Mediterranean experience increases in O₃ concentration in spring and autumn. Therefore,
655 although in the O₃ simulation, overall simulated GPP for Europe shows a small increase, large spatial variability

656 is shown in Fig's 4g &h because of the variability in O₃ concentration with region and season. Increased GPP
657 (dominantly 10%, but up to 20% in some areas) on 2001 levels is simulated across areas of Europe, however,
658 decreases of up to 21% are simulated in some areas of the Mediterranean, up to 15% in some areas of the boreal
659 region and up to 27% in the temperate zone (Fig. 4g & h).

660

661 When O₃ and CO₂ effects are combined (run_both_CO2+O3-simulation), simulated GPP increases (+15% to
662 +18%, high/low plant O₃ sensitivities respectively, Table 1). This increase is greater than the enhancement
663 simulated when CO₂ affects plant growth independently (run_CO2-simulation), because additional O₃ induced
664 stomatal closure increases soil water availability in some regions, which enhances growth more in ~~the~~
665 run_both_CO2+O3-simulation, compared to ~~the run_CO2-simulation~~. Nevertheless, although the percentage gain
666 is larger, the absolute value of GPP by 2050 remains lower in run_both_CO2+O3 compared to GPP in ~~the~~
667 run_CO2-simulations, highlighting the negative impact of O₃ at the land surface (Table S4).

668

669 Despite small increases in GPP in ~~the run_O3-simulation~~, the land carbon sink continues to decline from 2001
670 levels (-0.7% to -1.6%, low and high plant O₃ sensitivity respectively, Table 1). This is because the soil and
671 vegetation carbon pools continue to lose carbon as they adjust slowly to small changes in input (GPP), i.e. the soil
672 carbon pool is not in equilibrium in 2001, and is declining in response to reduced litter input as a result of 20th C
673 O₃ impacts on GPP. Nevertheless, the negative effect of O₃ on the future land sink is markedly reduced relative
674 to the historical period. Figure 4e & f however highlights regional differences. Boreal regions and parts of central
675 Europe see minimal O₃ damage, whereas some areas of southern and northern Europe see further losses of up to
676 8% on 2001 levels. The run_both_CO2+O3 simulation ~~isare~~ dominated by the physiological effects of changing
677 CO₂, with land carbon sink increases of up to 7% (Table 1).

678

679 3.5 European simulations – Full experimental period: 1901-2050

680

681 From 1901 to 2050, ~~the-run_O3-simulation~~ reduces GPP (-4% to -9%, with a significant difference between the
682 low and high plant O₃ sensitivity ($t=95$, $d.f.=6270$ $p<2.2e^{-16}$)) and land carbon storage (-3% to -7%, Table 1).
683 Regionally, O₃ damage is lowest in the boreal zone, GPP decreases are largely between 5% to 8% / 2% to 4% for
684 the high/low plant O₃ sensitivity respectively, with large areas minimally affected by O₃ damage (Figure 7),
685 consistent with lower g_s of needle leaf trees that dominate this region, and so lower O₃ uptake (Fig. ~~S17+6~~ &
686 ~~S18+7~~). In the temperate region, O₃ damage is extensive with reductions in GPP dominantly from 10% to 15%
687 for the low and high plant O₃ sensitivity respectively. Across significant areas of this region reductions in GPP
688 are up to 20% under high plant O₃ sensitivity (Figure 7). In the Mediterranean region, O₃ damage reduces GPP by
689 5% to 15% / 3% to 6% for the high/low plant O₃ sensitivity respectively, with some areas seeing greater losses of
690 up to 20% under the high plant O₃ sensitivity, but this is less extensive than that seen in the temperate zone (Figure
691 7). In these drier regions, O₃ induced stomatal closure can increase available soil moisture (Fig. ~~S17+6~~ & ~~S18+7~~).

692

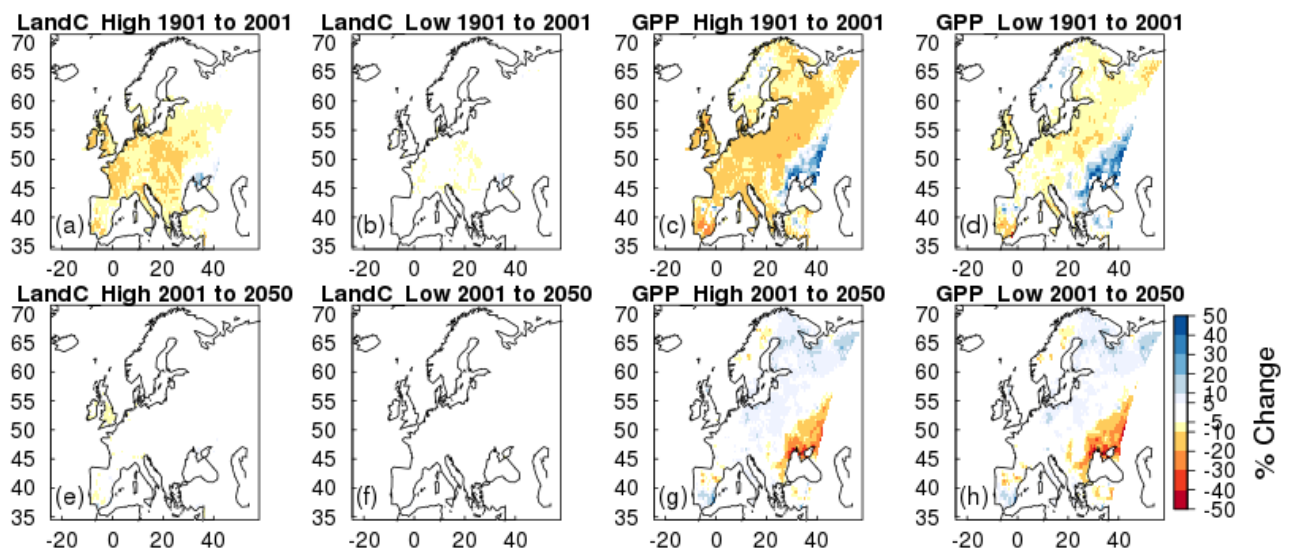
693 The run_both_CO2+O3 simulation shows that CO₂ induced stomatal closure can help alleviate O₃ damage by
694 reducing the uptake of O₃ (Table S6). In these simulations, CO₂-induced stomatal closure was found to offset O₃-
695 suppression of GPP, such that GPP by 2050 is 3% to 7% lower due to O₃ exposure (run_both_CO2+O3), rather

696 than 4% to 9% lower in the absence of increasing CO₂ (run_O3-simulation, Table S6). Figure 6 shows this
 697 spatially, O₃ damage is reduced when the effect of atmospheric CO₂ on stomatal closure is accounted for, however
 698 despite this, the land carbon sink and GPP remain significantly reduced due to O₃ exposure.

699

700 From 1901 to 2050, the-run_both_CO2+O3-simulation results in an increase in European land carbon uptake (+5%
 701 to +9%), and an increase in GPP (+20% to +23%) by 2050 for the high and low plant O₃ sensitivity, respectively
 702 (Table 1). Nevertheless, despite this increase there remains a large negative impact of O₃ on the European land
 703 carbon sink (Fig. S1948). By 2050 the simulated enhancement of land carbon and GPP in response to elevated
 704 CO₂ alone (run_CO2-simulation) is reduced by 3% to 6% (land carbon) and 4% to 9% (GPP) for the low and high
 705 plant O₃ sensitivity respectively, when O₃ is also accounted for (run_both_CO2+O33-simulation, Table 1). This
 706 is a large reduction in the ability of the European terrestrial biosphere to sequester carbon.

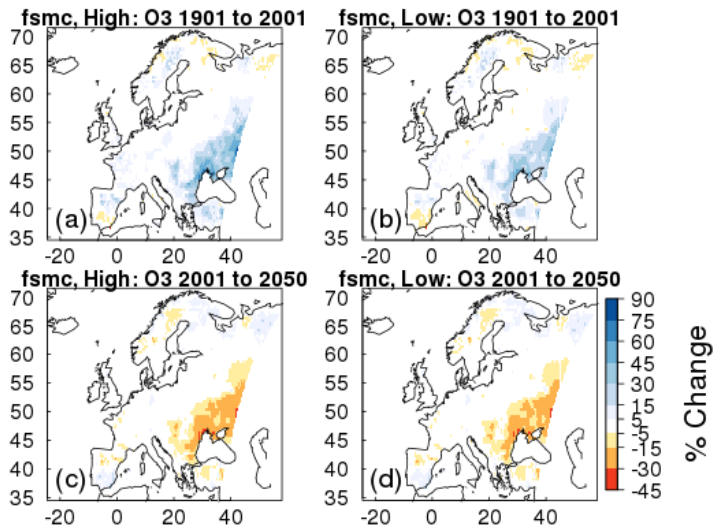
707



708

709 **Figure 4.** Simulated percentage change in total carbon stocks (Land C) and gross primary productivity (GPP) due
 710 to O₃ effects at fixed pre-industrial atmospheric CO₂ concentration (run_O3-simulation). Changes are shown for
 711 the periods 1901 to 2001, and 2001 to 2050 for the high and low plant O₃ sensitivity.

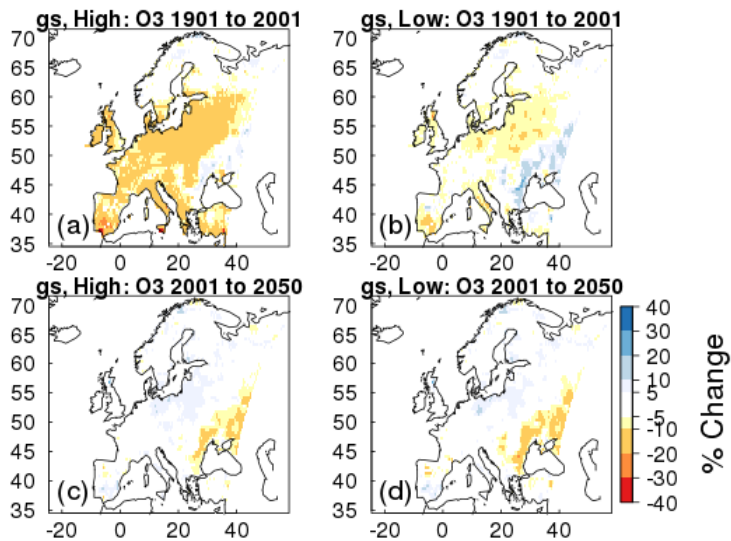
712



713

714 **Figure 5.** Simulated percentage change in plant available soil moisture (*fsmc*) due to O_3 effects at fixed pre-
 715 industrial atmospheric CO_2 concentration (run_ O_3 -simulation). Changes are shown for the periods 1901 to 2001,
 716 and 2001 to 2050 for the high and low plant O_3 sensitivity.

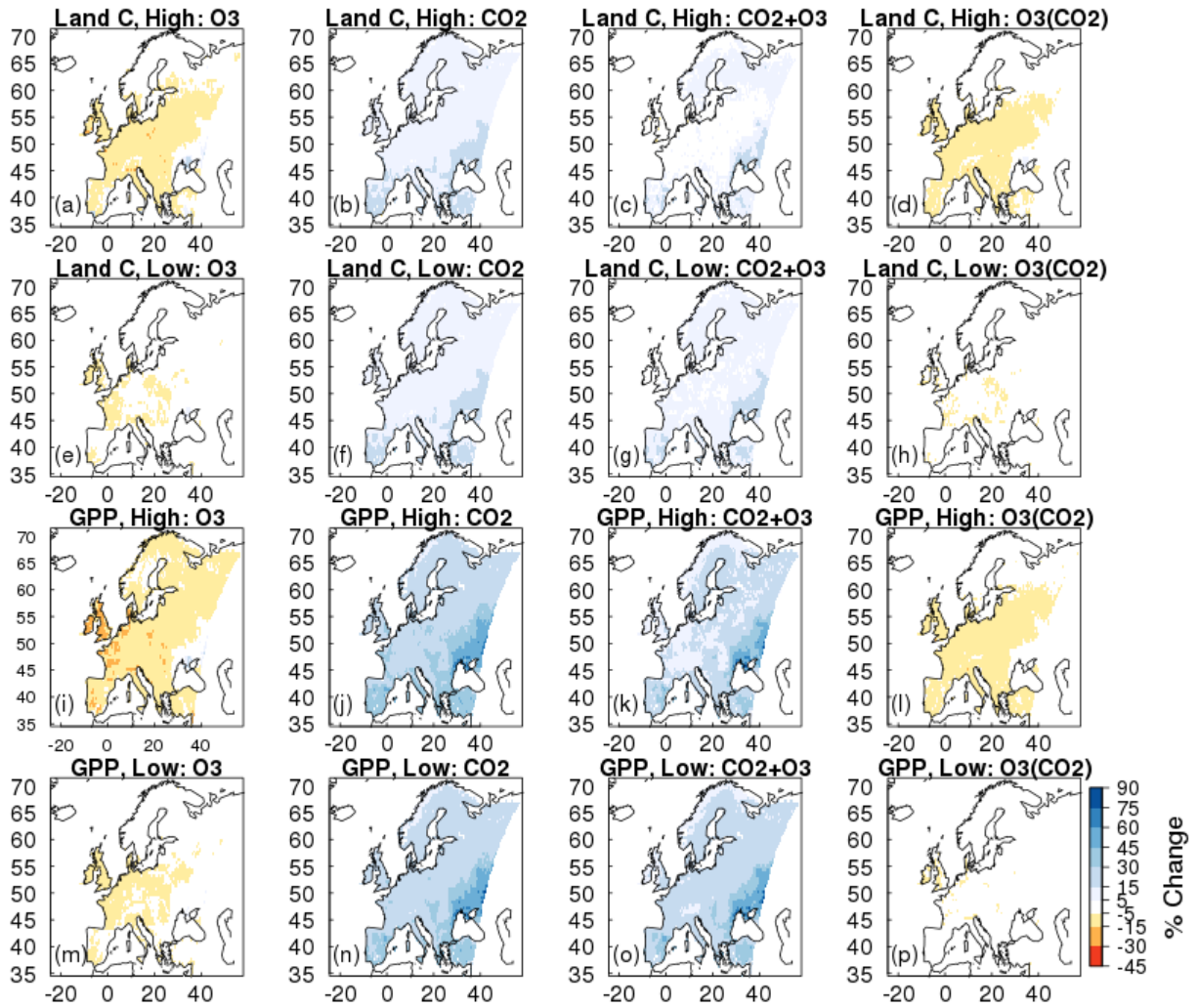
717



718

719 **Figure 6.** Simulated percentage change in stomatal conductance (g_s) due to O_3 effects at fixed pre-
 720 industrial atmospheric CO_2 concentration (run_ O_3 -simulation). Changes are shown for the periods 1901 to 2001,
 721 and 2001 to 2050 for the high and low plant O_3 sensitivity.

722



723

724 **Figure 7.** Simulated percentage change in total carbon stocks (Land C) and gross primary productivity (GPP) due to i) (a, e, i, m) O₃ effects at fixed pre-industrial atmospheric CO₂ concentration (run_O3-simulation), ii) (b, f, j, n) CO₂ fertilisation at fixed pre-industrial O₃ concentration (run_CO2-simulation), iii) (c, g, k, o) the interaction between O₃ and CO₂ effects (run_both_CO2+O3-simulation) iv) (d, h, l, p) O₃ effects with changing atmospheric CO₂ concentration (i.e. O₃ damage accounting for the effect of CO₂ induced stomatal closure; run_both_CO2+O3 - run_CO2). Changes are depicted for the periods 1901 to 2050 for high and lower ozone plant sensitivity.

730

731

732

733

734

735

736

	High Plant O ₃ Sensitivity					
	1901 - 2001		2001 - 2050		1901 - 2050	
	GPP (Pg C yr ⁻¹)	Land C (Pg C)	GPP (Pg C yr ⁻¹)	Land C (Pg C)	GPP (Pg C yr ⁻¹)	Land C (Pg C)
Value in 1901:	9.05	167	-	-	9.05	167
Absolute Change:						
O₃	-0.81	-9.21	0.01	-2.44	-0.80	-11.65
CO₂	1.16	4.24	1.42	12.98	2.58	17.22
CO₂ + O₃	0.13	-3.28	1.66	11.11	1.79	7.83
% Change:						
O₃	-8.95	-5.51	0.12	-1.55	-8.84	-6.98
CO₂	12.82	2.54	13.91	7.58	28.51	10.31
CO₂ + O₃	1.44	-1.96	18.08	6.79	19.78	4.69
	Low Plant O ₃ Sensitivity					
	1901 - 2001		2001 - 2050		1901 - 2050	
	GPP (Pg C yr ⁻¹)	Land C (Pg C)	GPP (Pg C yr ⁻¹)	Land C (Pg C)	GPP (Pg C yr ⁻¹)	Land C (Pg C)
Value in 1901:	9.34	167.5	-	-	9.34	167.5
Absolute Change:						
O₃	-0.30	-3.59	0.02	-1.07	-0.40	-4.66
CO₂	1.15	6.43	1.35	13.14	2.50	19.57
CO₂ + O₃	0.65	2.50	1.50	12.35	2.15	14.85
% Change:						
O₃	-3.21	-2.14	0.22	-0.65	-4.28	-2.78
CO₂	12.31	3.84	12.87	7.55	26.77	11.68
CO₂ + O₃	6.96	1.49	15.02	7.26	23.02	8.87

737

738 **Table 1.** Simulated changes in the European land carbon cycle due to changing O₃ and CO₂ concentrations
739 (independently and together). Shown are changes in total carbon stocks (Land C) and gross primary productivity
740 (GPP), over three different periods (historical: 1901 to 2001, future: 2001 to 2050, and full time series: 1901 to
741 2050). Absolute (top) and relative (bottom) differences are shown. For 2001 to 2050, please refer to Table S4 for
742 the initial value for each run. See the SI for details of the estimation of the O₃ and CO₂ effects and their interaction.

743

744

745

746

747

748

749

750

751

752

	Mean (Pg C)				
	1970-1979	1980-1989	1990-1999	2000-2009	2002-2011
Modelled O₃ effect on land C sink :					
Higher sensitivity	-1.32	-1.01	-0.97	-0.53	-0.50
Low sensitivity	-0.71	-0.58	-0.50	-0.29	-0.26
Sum of C emissions from fossil fuel combustion and cement production (Pg C)					
	8.39	8.63	12.26	12.83	12.75
C lost from O₃ effect as a % of fossil fuel and cement emissions (%):					
Higher sensitivity	-15.73	-11.70	-7.91	-4.13	-3.92
Low sensitivity	-8.46	-6.72	-4.08	-2.26	-2.04

753

754 **Table 2.** Simulated change in total land carbon due to O₃ damage with changing atmospheric CO₂ concentration
755 for the two vegetation sensitivities. The sum of carbon emissions for each decade from fossil fuel combustion and
756 cement production for the EU-28 countries plus Albania, Bosnia and Herzegovina, Iceland, Belarus, Serbia,
757 Moldova, Norway, Turkey, Ukraine, Switzerland and Macedonia (EU28-plus) are shown, the data is from Boden
758 *et al.*, 2013. The simulated change in land carbon as a result of O₃ damage is depicted as a percentage of the EU28-
759 plus emissions to demonstrate the magnitude of the additional source of carbon to the atmosphere from plant O₃
760 damage.

761

762 4 Discussion

763

764 4.1 Evaluation of g_s models and JULES O₃ model

765

766 Comparison of the new g_s model implemented in this study (MED) with the g_s model currently used as standard
767 in JULES (JAC) revealed large differences in g_s for each PFT, principally as a result of the data-based
768 parameterisation of the new model. Water use increased for the broadleaf tree and C₃ herbaceous PFTs using the
769 MED model compared to JAC, but decreased for the needle leaf tree, C₄ herbaceous and shrub PFTs which
770 displayed a more conservative water use strategy compared to JAC. These changes are in line with the work of
771 De Kauwe *et al.* (2015) who found a reduction in annual transpiration for evergreen needle leaf, tundra and C₄
772 grass regions when implementing the Medlyn g_s model into the Australian land surface scheme CABLE. Site-
773 level evaluation of the models against Fluxnet observations showed that in general the MED model improved
774 simulated seasonal cycles of latent and sensible heat. The magnitude of the improvement varied with site, **large**
775 improvements were seen at the deciduous savanna site, and at the NT sites and BT site (US_UMB) in the spring
776 and summer. However, much smaller improvements were seen at the grass sites. Changes in g_s in this study
777 resulted in differences in latent and sensible heat fluxes. Changes in the partitioning of energy fluxes at the land
778 surface could have consequences for the intensity of heatwaves (Cruz *et al.*, 2010; Kala *et al.*, 2016), runoff (Betts
779 *et al.*, 2007; Gedney *et al.*, 2006) and rainfall patterns (de Arellano *et al.*, 2012), although fully coupled simulations
780 would be necessary to detect these effects. The differences in simulated g_s led to differences in uptake of O₃
781 between the two models because the rate of g_s is the predominant determinant of the flux of O₃ through stomata.

782 Higher O₃ uptake is indicative of greater damage. Therefore, given that C₃ herbaceous vegetation is the dominant
783 land cover class across the European domain used in this study, this suggests a greater O₃ impact for Europe would
784 be simulated with MED model compared to JAC in our simulations where chemistry is uncoupled from the land
785 surface.

786

787 We evaluated the JULES O₃ model by comparing modelled GPP against the Jung et al (2011) MTE product.
788 Similar spatial patterns of GPP were simulated by JULES compared to MTE. Zonal means also showed similar
789 patterns of GPP, although JULES under predicted GPP compared to MTE at latitudes >45°N (temperate and boreal
790 regions; all simulations) and over predicted GPP at latitudes <45°N (Mediterranean region; all simulations). The
791 simulations with transient O₃ (i.e. O₃ and CO₂+O₃) showed large differences in GPP between the high and low
792 plant O₃ sensitivity simulations, this is to be expected given that the high plant O₃ sensitivity simulations were
793 parameterised to be ‘damaged’ more by O₃, i.e. greater reduction of photosynthesis/g_s with O₃ exposure compared
794 to the low plant O₃ sensitivity simulations. This difference was largest in the temperate zone, largely because of
795 C₃ grass cover being the dominant land cover here and the difference in the sensitivity to O₃ between the high and
796 low calibrations is significantly larger for C₃ grasses compared to the needle leaf trees that dominate in the boreal
797 region. Additionally, a longer growing season in the temperate region may allow for greater uptake of O₃ into
798 vegetation. C₃ grass is also the dominant land cover in the Mediterranean region with a different calibration used
799 for Mediterranean grasses for the low plant O₃ sensitivity which is less sensitive to O₃ than the temperate C₃
800 grasses, but high soil moisture stress is common throughout the growing season in the Mediterranean limiting the
801 uptake of O₃ through stomata, which likely diminishes the difference between the high and low calibrations. In
802 general, incorporating plant O₃ damage into JULES leads to worse agreement with the MTE GPP product,
803 however, this is expected to some degree as we are adding an explicit representation of O₃ damage to a model
804 calibrated to reproduce current day GPP and draw down of atmospheric CO₂. Inevitably this implicitly includes
805 O₃ damage to vegetation. Explicit representation of plant O₃ damage is important to investigate how O₃ damage
806 changes through time, under different emissions scenario’s, and the interactive effects with other gases (such as
807 CO₂) and with climate change. The percentage changes we simulate are therefore important to demonstrate the
808 sensitivity of modelled GPP and land Carbon to this process.

809

810 **4.2 ~~Lower than ex~~ Comparison of modelled estimates of O₃ damage?**

811

812 Our estimates suggest ~~present day~~ O₃ (run O₃) reduced GPP by 2001 by 3% to 9% on average across Europe and
813 NPP by 5% to 11% for the low and high plant O₃ sensitivities respectively-(Table S3). Anav et al. (2011) simulated
814 a 22% reduction of GPP across Europe for 2002 using the ORCHIDEE model. Present day O₃ exposure reduced
815 GPP by 10% to 25% in Europe, and 10.8% globally in the study by Lombardozzi et al. (2015) using the
816 Community land model (CLM). O₃ reduced NPP by 11.2% in Europe from 1989 to 1995 using the Terrestrial
817 Ecosystem Model (TEM) (Felzer et al., 2005). Globally, concentrations of O₃ predicted for 2100 reduced GPP by
818 14% to 23% using a former parameterisation of O₃ sensitivity in JULES (Sitch et al., 2007). The recent study by
819 Franz et al. (2017) showed mean GPP declined by 4.7% over the period 2001 to 2010 using the OCN model over

820 the same European domain and using the same O₃ forcing produced by EMEP MSC-W as used in this study. Our
821 estimates of changes in current day GPP and NPP are at the lower end of previously modelled estimates. Simulated
822 O₃ impacts will be dependent on model O₃ concentrations, meteorology, plant sensitivity to O₃, and process
823 representation of O₃ damage. Simulated O₃ impacts will depend in a large part on the scenario of O₃ concentrations
824 used as forcing, meteorological forcing and how sensitive vegetation is parameterised to be to O₃ damage, in
825 addition to the different process representation of O₃ damage in each model. It is therefore difficult to hypothesise
826 as to exactly why modelled estimates differ, but suggests that an ensemble approach to modelling O₃ impacts on
827 the terrestrial biosphere would be beneficial to understand some of these differences and provide estimates of O₃
828 damage with uncertainties.

829

830 **4.3 Impacts of O₃ at the land surface**

831

832 In this study, O₃ has a detrimental effect on the size of the land carbon sink for Europe. This is primarily through
833 a decrease in the size of the soil carbon pool as a result of reduced litter input to the soil, consistent with reduced
834 GPP/NPP. Field studies show that in some regions of Europe, soil carbon stocks are decreasing (Bellamy et al.,
835 2005;Capriel, 2013;Heikkinen et al., 2013;Sleutel et al., 2003). The study of Bellamy et al. (2005), for example,
836 showed that carbon was lost from soils across England and Wales between 1978 to 2003 at a mean rate of 0.6%
837 per year with little effect of land use on the rate of carbon loss, suggesting a possible link to climate change. It is
838 understood that climate change is likely to affect soil carbon turnover. Increased temperatures increase microbial
839 decomposition activity in the soil, and therefore increase carbon losses through higher rates of respiration (Cox et
840 al., 2000;Friedlingstein et al., 2006;Jones et al., 2003). However, some studies have found that O₃ can decrease
841 soil carbon content. Talhelm et al. (2014), for example, found O₃ reduced carbon content in near surface mineral
842 soil of forest soils exposed to 11 years of O₃ fumigation. Hofmockel et al. (2011) found elevated O₃ reduced the
843 carbon content in more stable soil organic matter pools, and Loya et al. (2003) showed that the fraction of soil
844 carbon formed in forest soils over a 4 year experimental period when fumigated with both CO₂ and O₃ was reduced
845 by 51% compared to the soil fumigated with CO₂ alone. It is agreed that amongst other factors that change with
846 O₃ exposure such as litter quality and composition, reduced litter quantity also has significant detrimental
847 consequences for soil carbon stocks (Andersen, 2003;Lindroth, 2010;Loya et al., 2003). Results from this study
848 therefore suggest that increasing tropospheric O₃ may be a contributing factor to the declining soil carbon stocks
849 observed across Europe as a result of reduced litter input to the soil carbon pool consistent with reduced NPP.

850

851 We acknowledge, however, that our model simulations do not include coupling of Nitrogen and Carbon cycles,
852 or land management practices. We include a representation of agricultural regions through the model calibration
853 against the wheat O₃ sensitivity function (CLRTAP, 2017), and in our simulations the high plant O₃ sensitivity
854 scenario uses this calibration against wheat for all C₃/C₄ land cover which dominates our model domain. Wheat is
855 known to be one of the most O₃ sensitive crop species however, so it is possible that our simulations over-estimate
856 the O₃ impact at the land surface. However, the low plant O₃ sensitivity calibration against natural grasslands
857 provides a counter estimate of the impact of O₃ at the land surface, therefore it is important to consider the range
858 our results provide (i.e. both the high and low plant O₃ sensitivity) as an indicator of the impact of O₃ on the land
859 surface. As with all uncoupled modelling studies, a change in g_s and flux will impact the O₃ concentration itself.

860 Therefore adopting the Medlyn formulation with a higher g_s and subsequently higher O_3 flux for broadleaf and C_3
861 PFTs (Fig 2) would lead to reduced O_3 concentration, which in turn ~~may would act to~~ dampen the effect of higher
862 g_s on O_3 flux, although the higher uptake of O_3 by vegetation may lead to more damage and increase O_3
863 concentrations, in an uncoupled chemistry-land modelling system such as this it is not possible to predict which
864 process would dominate. Additionally, this version of JULES does not have a crop module; it has no land
865 management practices such as harvesting, ploughing or crop rotation – processes which may have counteracting
866 effects on the land carbon sink. Further, without a coupled Carbon and Nitrogen cycle, it is likely that the CO_2
867 fertilisation response of GPP and the land carbon sink is over estimated in some regions of our simulations since
868 nitrogen availability limits terrestrial carbon sequestration of natural ecosystems in the temperate and boreal zone
869 (Zaehle, 2013). This would have consequences for our modelled O_3 impact, particularly into the future where the
870 large CO_2 fertilisation effect was responsible for partly offsetting the negative impact of O_3 . Although in our
871 simulations a high fraction of land cover is agricultural which we assume would be optimally fertilised. Our
872 simulations also use a fixed climate, so we do not include the effect of climate change on shifting plant phenology.
873 Therefore, our results may underestimate plant O_3 damage, since if the growing season started earlier or finished
874 later, plants in some regions would be exposed to higher O_3 concentrations. Nevertheless, we emphasise that this
875 study provides a sensitivity assessment of the impact of plant O_3 damage on GPP and the land carbon sink.

876
877 Another caveat we fully acknowledge is that at the leaf-level JULES is parameterised to reduce g_s with O_3
878 exposure. Whilst this response is commonly observed (Wittig et al., 2007; Ainsworth et al., 2012), there is evidence
879 to suggest that O_3 impairs stomata in some species, making them non-responsive to environmental stimuli (Hayes
880 et al., 2012; Hoshika et al., 2012a; Mills et al., 2009; Paoletti and Grulke, 2010). In drought conditions the
881 mechanism is thought to involve O_3 stimulated ethylene production which interferes with the stomatal response
882 to ABA signalling (Wilkinson and Davies, 2009; Wilkinson and Davies, 2010). Such stomatal sluggishness can
883 result in higher O_3 uptake and injury, increased water-loss, and therefore greater vulnerability to environmental
884 stresses (Mills et al., 2016). McLaughlin (2007a; 2007b) and Sun et al. (2012) provide evidence of increased
885 transpiration and reduced streamflow in forests at the regional scale in response to ambient levels of O_3 , and
886 suggest this could increase the frequency and severity of droughts. Hoshika et al. (2012b) however found that
887 despite sluggish stomatal control in O_3 exposed trees, whole tree water use was lower in these trees because of
888 lower gas exchange and premature leaf shedding of injured leaves. To our knowledge, the study of Hoshika et al.
889 (2015) is the first to include an explicit representation of sluggish stomatal control in a land-atmosphere model,
890 they show that sluggish stomatal behaviour has implications for carbon and water cycling in ecosystems.
891 However, it is by no means a ubiquitous response, and it is not fully understood which species respond this way
892 and under what conditions (Mills et al., 2016; Wittig et al., 2007). Nevertheless, this remains an important area of
893 future work.

894
895 In this work we implement the stomatal closure proposed in Medlyn et al., (2011), this uses the parameter g_l .
896 Hoshika et al. (2013) show a significant difference in the g_l parameter (higher in elevated O_3 compared to ambient)
897 in Siebold's beech in June of their experiment. However, this is only at the start of the growing season, further
898 measurements show no difference in this parameter between O_3 treatments. Quantifying an O_3 effect directly on
899 g_l would require a detailed meta-analysis of empirical data on photosynthesis and g_s for different PFTs, which is

900 currently lacking in the literature. ~~With such information lacking, here we take an empirical approach to modelling~~
901 ~~plant O₃ damage, essentially by applying a reduction factor to the simulated plant photosynthesis based on~~
902 ~~observations of whole plant losses of biomass with accumulated O₃ exposure, for which there is a lot more~~
903 ~~available data (e.g. CLRTAP, 2017).~~

904
905
906 A further caveat of this study is that the O₃ concentrations used to force the model are offline, in this case generated
907 by the EMEP MSC-W model. This means the depositional sink is different in JULES (Medlyn formulation),
908 compared to the EMEP model which uses the g_s formulation presented in Emberson et al. (2000) and Emberson
909 et al. (2001). Because we link two different model systems, the g_s values in the EMEP model differ from those
910 obtained using the Medlyn formulation, which would ultimately lead to different O₃ concentrations. The role of
911 EMEP in this study is to provide O₃ concentrations at the top of the vegetation canopy to force JULES and not g_s,
912 how the different depositional sinks would affect simulated O₃ concentrations at canopy height has not been
913 investigated.

914 ~~The calculation of O₃ deposition in the EMEP model uses the stomatal conductance formulation~~
915 ~~presented in Emberson et al., which depends on temperature, light, humidity and soil moisture~~
916 ~~(commonly referred to as DO₃SE). Because we link two different model systems, the g_s values in the~~
917 ~~EMEP model differ from those obtained using the Medlyn formulation. We acknowledge this~~
918 ~~inconsistency as a caveat of our study, however comparison of g_{max} (maximum g_s) values from both~~
919 ~~models (EMEP (g_{max} is an input parameter determining the maximum g_s) and JULES (g_{max} is not~~
920 ~~used as an input parameter in JULES, instead we calculated g_{max} for each PFT taking the mean across~~
921 ~~the model domain for the year 2001) suggests the differences are small for deciduous forest (EMEP~~
922 ~~150-200, JULES ~180, all units in mmol O₃/m²-(PLA)/s), and C₃/C₄ crops (EMEP 270-300, JULES~~
923 ~~~260-390), but are larger for coniferous forest (EMEP 140-200, JULES ~60-70) and shrubs (EMEP 60-~~
924 ~~200, JULES 360-390). It should be noted that the role of EMEP in this study is not to provide g_s, but~~
925 ~~to provide O₃ at the top of the vegetation canopy. This firstly entails a calculation of the large-scale~~
926 ~~ozone concentrations for Europe, which are represented by the gridded values of grid-cell average~~
927 ~~concentration, and secondly to calculate the vertical gradients between these grid-cell centres (at ca.~~
928 ~~45m) and the top of the vegetation canopy. O₃ deposition is important for both steps; it is known to~~
929 ~~have a substantial impact on the lifetime and concentrations of O₃ in the planetary boundary layer~~
930 ~~(Garland and Derwent, 1979; Val Martin et al., 2014), and also in determining the local vertical gradients~~
931 ~~above different land-covers (CLRTAP, 2017; Gerosa et al., 2017; Tuovinen et al., 2009). Vertical~~
932 ~~gradients between the 45m level and the top of forest canopies tend to be limited (Fuentes et al.,~~
933 ~~2007; Karlsson et al., 2006) due to the good mixing normally induced by forest roughness. Vertical~~
934 ~~gradients between 45m and the top of shorter vegetation such as grasslands or crops can be larger~~
935 ~~however (CLRTAP, 2017; Gerosa et al., 2017). Accounting for such land-cover specific gradient effects~~
936 ~~has been shown to have large impacts on estimates of O₃ metrics (Simpson et al., 2007).~~

937

938 These offline simulations show the sensitivity of GPP and the land carbon sink to tropospheric O₃, suggesting that
939 O₃ is an important predictor of future GPP and the land carbon store across Europe. There are uncertainties in our
940 estimates however from the use of uncoupled tropospheric chemistry, meteorology and stomatal function. For
941 example, increased frequency of drought in the future would reduce stomatal conductance (assuming no sluggish
942 stomatal response) and thus O₃ uptake. Since our offline simulations do not include this feedback it is possible the
943 O₃ effect is over estimated here. Given the complexity of potential interactions and feedbacks it remains difficult
944 to diagnose the importance of individual factors (e.g. the direct physiological response) in a fully coupled
945 simulation. Once the importance of a process is demonstrated offline, it provides evidence of the need to
946 incorporate such process in coupled regional and global simulations.

947

948 **4.4 O₃ as a missing component of carbon cycle assessments?**

949

950 Comprehensive analyses of the European carbon balance suggest a large biogenic carbon sink (Janssens et al.,
951 2003;Luyssaert et al., 2012;Schulze et al., 2009). However, estimates are hampered by large uncertainties in key
952 components of the land carbon balance, such as estimates of soil carbon gains and losses (Ciais et al.,
953 2010;Janssens et al., 2003;Schulze et al., 2009;Schulze et al., 2010). We suggest that the effect of O₃ on plant
954 physiology is a contributing factor to the decline in soil carbon stores observed across Europe, and as such this O₃
955 effect is a missing component of European carbon cycle assessments. Over the full experimental period (1901 to
956 2050), our results show elevated O₃ concentrations reduce the amount of carbon that can be stored in the soil by
957 3% to 9% (low and high plant O₃ sensitivity, respectively), which almost completely offsets the beneficial effects
958 of CO₂ fertilisation on soil carbon storage under the high plant O₃ sensitivity . This would contribute to a change
959 in the size of a key carbon sink for Europe, and is particularly important when we consider the evolution of the
960 land carbon sink into the future given the impact of O₃ on soil carbon sequestration and the high uncertainty of
961 future tropospheric O₃ concentrations. Schulze et al. (2009) and Luyssaert et al. (2012) extended their analysis of
962 the European carbon balance to include additional non-CO₂ greenhouse gases (CH₄ and N₂O). Both studies found
963 that emissions of these offset the biogenic carbon sink, reducing the climate mitigation potential of European
964 ecosystems. This highlights the importance of accounting for all fluxes and stores in carbon/greenhouse gas
965 balance assessments, of which O₃ and its indirect effect on the CO₂ flux via direct effects on plant physiology is
966 currently missing.

967

968 **4.5 ~~The interactive effects of~~Interactive effects ofbetween O₃ and CO₂**

969

970 We looked at the ~~interactive effects ofinteraction between~~ ~~CO₂ and O₃-effects~~. Our results support the hypothesis
971 that elevated atmospheric CO₂ provides some protection against O₃ damage because of lower g_s that reduces
972 uptake of O₃ through stomata (Harmens et al., 2007;Wittig et al., 2007). In the present study, reductions in GPP
973 and the land carbon store due to O₃ exposure were lower when simulated with concurrent changes in atmospheric
974 CO₂. Despite acclimation of photosynthesis after long-term exposure to elevated atmospheric CO₂ of field grown
975 plants (Ainsworth and Long, 2005;Medlyn et al., 1999), there is no evidence to suggest that g_s acclimates
976 (Ainsworth et al., 2003;Medlyn et al., 2001). This suggests the protective effect of elevated atmospheric CO₂
977 against O₃ damage will be sustained in the long term. However, although meta-analysis suggest a general trend

978 of reduced g_s with elevated CO_2 (Ainsworth and Long, 2005;Medlyn et al., 1999), this is not a universal response.
979 Stomatal responses on exposure to elevated CO_2 with FACE treatment varied with genotype and growth stage in
980 a fast-growing poplar community (Bernacchi et al., 2003;Tricker et al., 2009). In other mature forest stands,
981 limited stomatal response to elevated CO_2 was observed after canopy closure (Ellsworth, 1999;Uddling et al.,
982 2009). Also, some studies found that stomatal responses to CO_2 were significant only under high atmospheric
983 humidity (Cech et al., 2003;Leuzinger and Körner, 2007;Wullschleger et al., 2002). These examples illustrate that
984 stomatal responses to elevated atmospheric CO_2 are not universal, and as such the protective effect of CO_2 against
985 O_3 injury cannot be assumed for all species, at all growth stages under wide ranging environmental conditions.

986

987 **5 Conclusion**

988

989 What is abundantly clear is that plant responses to both CO_2 and O_3 are complicated by a host of factors that are
990 only partly understood, and it remains difficult to identify general, global patterns given that effects of both gases
991 on plant communities and ecological interactions are highly context and species specific (Ainsworth and Long,
992 2005;Fuhrer et al., 2016;Matyssek et al., 2010b). This study quantifies the sensitivity of the land carbon sink for
993 Europe and GPP to changing concentrations of atmospheric CO_2 and O_3 from 1901 to 2050. We have used a state
994 of the art land surface model calibrated for European vegetation to give our best estimates of this sensitivity within
995 the limits of data availability to calibrate the model for O_3 sensitivity, current knowledge and model structure. In
996 summary, this study has shown that potential gains in terrestrial carbon sequestration over Europe resulting from
997 elevated CO_2 can be partially offset by concurrent rises in tropospheric O_3 over 1901-2050. Specifically, we have
998 shown that the negative effect of O_3 on the land carbon sink was greatest over the twentieth century, when O_3
999 concentrations increased rapidly from pre-industrial levels. Over this period soil carbon stocks were diminished
1000 over agricultural areas, consistent with reduced NPP and litter input. This loss of soil carbon was largely
1001 responsible for the decrease in the size of the land carbon sink over Europe. The O_3 effect on the land carbon store
1002 and flux was reduced into the future as CO_2 concentration rose considerably and changes in O_3 concentration were
1003 less pronounced. However, there remained a large cumulative negative impact on the land carbon sink for Europe
1004 by 2050. The interaction between the two gases was found to reduce O_3 injury owing to reduced stomatal opening
1005 in elevated atmospheric CO_2 . However, primary productivity and land carbon storage remained suppressed by
1006 2050 due to plant O_3 damage. Expressed as a percentage of the emissions from fossil fuel and cement production
1007 for the EU28-plus countries, the carbon emissions from O_3 -induced plant injury are a source of anthropogenic
1008 carbon previously not accounted for in carbon cycle assessments. Our results demonstrate the sensitivity of
1009 modelled terrestrial carbon dynamics to the direct effect of tropospheric O_3 and its interaction with atmospheric
1010 CO_2 on plant physiology, demonstrating this process is an important predictor of future GPP and trends in the
1011 land-carbon sink. Nevertheless, this process remains largely unconsidered in regional and global climate model
1012 simulations that are used to model carbon sources and sinks and carbon-climate feedbacks.

1013

1014

1015

1016 **Data availability**

1017

1018 The JULES model can be downloaded from the Met Office Science Repository Service
1019 (<https://code.metoffice.gov.uk/trac/jules> - see here for a helpful how to [http://jules.jchmr.org/content/getting-](http://jules.jchmr.org/content/getting-started)
1020 started). Model output data presented in this paper and the exact version of JULES with namelists are available
1021 upon request from the corresponding author.

1022

1023 **Supplementary Information**

1024

1025 Supplementary_Information_Oliver_et_al_vn4.0.docx

1026

1027 **Competing Interests**

1028 The authors declare that they have no conflict of interest

1029

1030 **Acknowledgements**

1031

1032 RJO and LMM were supported by the EU FP7 (ECLAIRE, 282910) and JWCRP (UKESM, NEC05816). This
1033 work was also supported by EMEP under UNECE. SS and LMM acknowledge the support of the NERC
1034 SAMBBA project (NE/J010057/1). The UK Met Office contribution was funded by BEIS under the Hadley Centre
1035 Climate Programme (GA01101). GAF also acknowledges funding from the EU's Horizon 2020 research and
1036 innovation programme (CRESCENDO, 641816). We also thank Magnus Engardt of SMHI for providing the
1037 RCA3 climate dataset. This work used eddy covariance data acquired and shared by the FLUXNET community,
1038 including these networks: AmeriFlux, AfriFlux, AsiaFlux, CarboAfrica, CarboEuropeIP, CarboItaly, CarboMont,
1039 ChinaFlux, Fluxnet-Canada, GreenGrass, ICOS, KoFlux, LBA, NECC, OzFlux-TERN, TCOS-Siberia, and
1040 USCCC. The ERA-Interim reanalysis data are provided by ECMWF and processed by LSCE. The FLUXNET
1041 eddy covariance data processing and harmonization was carried out by the European Fluxes Database Cluster,
1042 AmeriFlux Management Project, and Fluxdata project of FLUXNET, with the support of CDIAC and ICOS
1043 Ecosystem Thematic Center, and the OzFlux, ChinaFlux and AsiaFlux offices. We also thank the two anonymous
1044 reviewers who helped to improve this manuscript.

1045

1046

1047 **References**

1048

1049 Ainsworth, E., and Long, S.: What have we learned from 15 years of free-air CO₂ enrichment (FACE)?
1050 A meta-analytic review of the responses of photosynthesis, canopy properties and plant production
1051 to rising CO₂, *New Phytologist*, 165, 351-372, 2005.
1052 Ainsworth, E. A., Davey, P. A., Hymus, G. J., Osborne, C. P., Rogers, A., Blum, H., Nosberger, J., and
1053 Long, S. P.: Is stimulation of leaf photosynthesis by elevated carbon dioxide concentration
1054 maintained in the long term? A test with *Lolium perenne* grown for 10 years at two nitrogen
1055 fertilization levels under Free Air CO₂ Enrichment (FACE), *Plant, Cell and Environment*, 26, 705-714,
1056 2003.

1057 Ainsworth, E. A.: Rice production in a changing climate: a meta-analysis of responses to elevated
1058 carbon dioxide and elevated ozone concentration, *Global Change Biology*, 14, 1642-1650,
1059 10.1111/j.1365-2486.2008.01594.x, 2008.

1060 Ainsworth, E. A., Yendrek, C. R., Sitch, S., Collins, W. J., and Emberson, L. D.: The Effects of
1061 Tropospheric Ozone on Net Primary Productivity and Implications for Climate Change, *Annual*
1062 *Review of Plant Biology*, 63, 637-661, doi:10.1146/annurev-arplant-042110-103829, 2012.

1063 Anav, A., Menut, L., Khvorostyanov, D., and Viovy, N.: Impact of tropospheric ozone on the Euro-
1064 Mediterranean vegetation, *Global change biology*, 17, 2342-2359, 2011.

1065 Andersen, C. P.: Source-sink balance and carbon allocation below ground in plants exposed to
1066 ozone, *New Phytologist*, 157, 213-228, 10.1046/j.1469-8137.2003.00674.x, 2003.

1067 Arneth, A., Harrison, S. P., Zaehle, S., Tsigaridis, K., Menon, S., Bartlein, P. J., Feichter, J., Korhola, A.,
1068 Kulmala, M., O'Donnell, D., Schurgers, G., Sorvari, S., and Vesala, T.: Terrestrial biogeochemical
1069 feedbacks in the climate system, *Nature Geosci*, 3, 525-532,
1070 http://www.nature.com/ngeo/journal/v3/n8/supinfo/ngeo905_S1.html, 2010.

1071 Auvray, M., and Bey, I.: Long-range transport to Europe: Seasonal variations and implications for the
1072 European ozone budget, *Journal of Geophysical Research: Atmospheres*, 110,
1073 doi:10.1029/2004JD005503, 2005.

1074 Avnery, S., Mauzerall, D. L., Liu, J., and Horowitz, L. W.: Global crop yield reductions due to surface
1075 ozone exposure: 1. Year 2000 crop production losses and economic damage, *Atmospheric*
1076 *Environment*, 45, 2284-2296, <https://doi.org/10.1016/j.atmosenv.2010.11.045>, 2011.

1077 Baig, S., Medlyn, B. E., Mercado, L. M., and Zaehle, S.: Does the growth response of woody plants to
1078 elevated CO₂ increase with temperature? A model-oriented meta-analysis, *Global Change Biology*,
1079 21, 4303-4319, 10.1111/gcb.12962, 2015.

1080 Bellamy, P. H., Loveland, P. J., Bradley, R. I., Lark, R. M., and Kirk, G. J.: Carbon losses from all soils
1081 across England and Wales 1978-2003, *Nature*, 437, 245-248, 2005.

1082 Bernacchi, C. J., Calfapietra, C., Davey, P. A., Wittig, V. E., Scarascia-Mugnozza, G. E., Raines, C. A.,
1083 and Long, S. P.: Photosynthesis and stomatal conductance responses of poplars to free-air CO₂
1084 enrichment (PopFACE) during the first growth cycle and immediately following coppice., *New*
1085 *Phytologist*, 159, 609-621, 2003.

1086 Best, M. J., Pryor, M., Clark, D. B., Rooney, G. G., Essery, R. L. H., Menard, C. B., Edwards, J. M.,
1087 Hendry, M. A., Porson, N., Gedney, N., Mercado, L. M., Sitch, S., Blyth, E., Boucher, O., Cox, P. M.,
1088 Grimmond, C. S. B., and Harding, R. J.: The Joint UK Land Environment Simulator (JULES), Model
1089 description - Part 1: Energy and water fluxes, *Geoscientific Model Development Discussions*, 4, 595-
1090 640, 10.5194/GMDD-4-595-2011, 2011.

1091 Betts, R. A., Boucher, O., Collins, M., Cox, P. M., Falloon, P. D., Gedney, N., Hemming, D. L.,
1092 Huntingford, C., Jones, C. D., and Sexton, D. M.: Projected increase in continental runoff due to plant
1093 responses to increasing carbon dioxide, *Nature*, 448, 1037-1041, 2007.

1094 Boden, T. A., Marland, G., and Andres, R. J.: Global, Regional, and National Fossil-Fuel CO₂ Emissions,
1095 Oak Ridge National Laboratory, U.S. Department of Energy, Oak Ridge, Tenn., USA, 2013.

1096 Büker, P., Feng, Z., Uddling, J., Briolat, A., Alonso, R., Braun, S., Elvira, S., Gerosa, G., Karlsson, P. E.,
1097 Le Thiec, D., Marzuoli, R., Mills, G., Oksanen, E., Wieser, G., Wilkinson, M., and Emberson, L. D.: New
1098 flux based dose-response relationships for ozone for European forest tree species, *Environmental*
1099 *Pollution*, 163-174, 2015.

1100 Calvete-Sogo, H., Elvira, S., Sanz, J., González-Fernández, I., García-Gómez, H., Sánchez-Martín, L.,
1101 Alonso, R., and Bermejo-Bermejo, V.: Current ozone levels threaten gross primary production and
1102 yield of Mediterranean annual pastures and nitrogen modulates the response, *Atmospheric*
1103 *Environment*, 95, 197-206, <http://dx.doi.org/10.1016/j.atmosenv.2014.05.073>, 2014.

1104 Capriel, P.: Trends in organic carbon and nitrogen contents in agricultural soils in Bavaria (south
1105 Germany) between 1986 and 2007, *European Journal of Soil Science*, 64, 445-454, 2013.

1106 Cech, P. G., Pepin, S., and Korner, C.: Elevated CO₂ reduces sap flux in mature deciduous forest trees,
1107 *Oecologia*, 137, 258-268, 2003.

1108 Ceulemans, R., and Mousseau, M.: Effects of elevated atmospheric CO₂ on woody plants, *New*
1109 *Phytologist*, 127, 1994.

1110 Ciais, P., Wattenbach, M., Vuichard, N., Smith, P., Piao, S., Don, A., Luyssaert, S., Janssens, I.,
1111 Bondeau, A., and Dechow, R.: The European carbon balance. Part 2: croplands, *Global Change*
1112 *Biology*, 16, 1409-1428, 2010.

1113 Ciais, P., Sabine, C., Bala, G., Bopp, L., Brovkin, V., Canadell, J., Chhabra, A., DeFries, R., Galloway, J.,
1114 Heimann, M., Jones, C., Le Quéré, C., Myneni, R. B., Piao, S., and Thornton, P.: Carbon and Other
1115 Biogeochemical Cycles. In: *Climate Change 2013: The Physical Science Basis. Contribution of Working*
1116 *Group I to the Fifth Assessment Report of the Intergovernmental Panel on Climate Change* [Stocker,
1117 T.F., D. Qin, G.-K. Plattner, M. Tignor, S.K. Allen, J. Boschung, A. Nauels, Y. Xia, V. Bex and P.M.
1118 Midgley (eds.)]. Cambridge University Press, Cambridge, United Kingdom and New York, NY, USA.,
1119 2013.

1120 Clark, D. B., Mercado, L. M., Sitch, S., Jones, C. D., Gedney, N., Best, M. J., Pryor, M., Rooney, G. G.,
1121 Essery, R. L. H., Blyth, E., Boucher, O., Harding, R. J., and Cox, P. M.: The Joint UK Land Environment
1122 Simulator (JULES), Model description - Part 2: Carbon fluxes and vegetation, *Geoscientific Model*
1123 *Development Discussions*, 4, 641-688, 10.5194/gmdd-4-641-2011, 2011.

1124 CLRTAP: The UNECE Convention on Long-range Transboundary Air Pollution. Manual on
1125 Methodologies and Criteria for Modelling and Mapping Critical Loads and Levels and Air Pollution
1126 Effects, Risks and Trends: Chapter III Mapping Critical Levels for Vegetation, accessed via,
1127 [http://icpvegetation.ceh.ac.uk/publications/documents/Chapter3-](http://icpvegetation.ceh.ac.uk/publications/documents/Chapter3-Mappingcriticallevelsforvegetation_000.pdf)
1128 [Mappingcriticallevelsforvegetation_000.pdf](http://icpvegetation.ceh.ac.uk/publications/documents/Chapter3-Mappingcriticallevelsforvegetation_000.pdf), 2017.

1129 Collins, W. J., Sitch, S., and Boucher, O.: How vegetation impacts affect climate metrics for ozone
1130 precursors, *Journal of Geophysical Research: Atmospheres*, 115, D23308, 10.1029/2010JD014187,
1131 2010.

1132 Collins, W. J., Bellouin, N., Doutriaux-Boucher, M., Gedney, N., Halloran, P., Hinton, T., Hughes, J.,
1133 Jones, C. D., Joshi, M., Liddicoat, S., Martin, G., O'Connor, F., Rae, J., Senior, C., Sitch, S., Totterdell, I.,
1134 Wiltshire, A., and Woodward, S.: Development and evaluation of an Earth-System model –
1135 HadGEM2, *Geosci. Model Dev.*, 4, 1051-1075, 10.5194/gmd-4-1051-2011, 2011.

1136 Cooper, O. R., Parrish, D. D., Stohl, A., Trainer, M., Nedelec, P., Thouret, V., Cammas, J. P., Oltmans,
1137 S. J., Johnson, B. J., Tarasick, D., Leblanc, T., McDerimid, I. S., Jaffe, D., Gao, R., Stith, J., Ryerson, T.,
1138 Aikin, K., Campos, T., Weinheimer, A., and Avery, M. A.: Increasing springtime ozone mixing ratios in
1139 the free troposphere over western North America, *Nature*, 463, 344-348,
1140 http://www.nature.com/nature/journal/v463/n7279/supinfo/nature08708_S1.html, 2010.

1141 Cooper, O. R., Parrish, D., Ziemke, J., Balashov, N., Cupeiro, M., Galbally, I., Gilge, S., Horowitz, L.,
1142 Jensen, N., and Lamarque, J.-F.: Global distribution and trends of tropospheric ozone: An
1143 observation-based review, *Elementa: Science of the Anthropocene*, 2, 000029, 2014.

1144 Cox, P. M., Betts, R. A., Jones, C. D., Spall, S. A., and Totterdell, I. J.: Acceleration of global warming
1145 due to carbon-cycle feedbacks in a coupled climate model, *Nature*, 408, 184-187, 2000.

1146 Cox, P. M.: Description of the TRIFFID dynamic global vegetation model, Hadley Centre technical
1147 note 24, 2001.

1148 Cruz, F. T., Pitman, A. J., and Wang, Y. P.: Can the stomatal response to higher atmospheric carbon
1149 dioxide explain the unusual temperatures during the 2002 Murray-Darling Basin drought?, *Journal of*
1150 *Geophysical Research: Atmospheres*, 115, 2010.

1151 de Arellano, J. V.-G., van Heerwaarden, C. C., and Lelieveld, J.: Modelled suppression of boundary-
1152 layer clouds by plants in a CO₂-rich atmosphere, *Nature geoscience*, 5, 701-704, 2012.

1153 De Kauwe, M., Kala, J., Lin, Y.-S., Pitman, A., Medlyn, B., Duursma, R., Abramowitz, G., Wang, Y.-P.,
1154 and Miralles, D.: A test of an optimal stomatal conductance scheme within the CABLE land surface
1155 model, 8, 431-452, 2015.

1156 Derwent, R. G., Stevenson, D. S., Doherty, R. M., Collins, W. J., Sanderson, M. G., and Johnson, C. E.:
1157 Radiative forcing from surface NO_x emissions: spatial and seasonal variations, *Climatic Change*, 88,
1158 385-401, 10.1007/s10584-007-9383-8, 2008.

1159 Derwent, R. G., Utembe, S. R., Jenkin, M. E., and Shallcross, D. E.: Tropospheric ozone production
1160 regions and the intercontinental origins of surface ozone over Europe, *Atmospheric Environment*,
1161 112, 216-224, <https://doi.org/10.1016/j.atmosenv.2015.04.049>, 2015.

1162 Ellsworth, D. S.: CO₂ enrichment in a maturing pine forest: are CO₂ exchange and water status in the
1163 canopy affected?, *Plant, Cell and Environment*, 22, 461-472, 1999.

1164 Emberson, L. D., Ashmore, M. R., Cambridge, H. M., Simpson, D., and Tuovinen, J.-P.: Modelling
1165 stomatal ozone flux across Europe, *Environmental Pollution*, 109, 403–413, 2000.

1166 Emberson, L. D., Simpson, D., Tuovinen, J.-P., Ashmore, M. R., and Cambridge, H. M.: Modelling and
1167 mapping ozone deposition in Europe, *Water Air Soil Pollution*, 130, 577–582, 2001.

1168 Emberson, L. D., Büker, P., and Ashmore, M. R.: Assessing the risk caused by ground level ozone to
1169 European forest trees: A case study in pine, beech and oak across different climate regions,
1170 *Environmental Pollution*, 147, 454–466, 2007.

1171 Engardt, M., Simpson, D., Schwikowski, M., and Granat, L.: Deposition of sulphur and nitrogen in
1172 Europe 1900-2050. Model calculations and comparison to historical observations, *Tellus B: Chem.*
1173 *Phys. Meteor.*, 69, 2017.

1174 Etheridge, D. M., Steele, L. P., Langenfelds, R. L., Francey, R. J., M., B., and Morgan, V. I.: Natural and
1175 anthropogenic changes in atmospheric CO₂ over the last 1000 years from air in Antarctic ice and firn,
1176 *Journal of Geophysical Research*, 101(D2), 4115–4128, doi:10.1029/95JD03410, 1996.

1177 Fagnano, M., Maggio, A., and Fumagalli, I.: Crops' responses to ozone in Mediterranean
1178 environments, *Environmental Pollution*, 157, 1438-1444, 2009.

1179 Fares, S., Vargas, R., Detto, M., Goldstein, A. H., Karlik, J., Paoletti, E., and Vitale, M.: Tropospheric
1180 ozone reduces carbon assimilation in trees: estimates from analysis of continuous flux
1181 measurements, *Global change biology*, 19, 2427-2443, 2013.

1182 Felzer, B., Reilly, J., Melillo, J., Kicklighter, D., Sarofim, M., Wang, C., Prinn, R., and Zhuang, Q.: Future
1183 Effects of Ozone on Carbon Sequestration and Climate Change Policy Using a Global Biogeochemical
1184 Model, *Climatic Change*, 73, 345-373, 10.1007/s10584-005-6776-4, 2005.

1185 Felzer, B. S. F., Kicklighter, D. W., Melillo, J. M., Wang, C., Zhuang, Q., and Prinn, R. G.: Ozone effects
1186 on net primary productivity and carbon sequestration in the conterminous United States using a
1187 biogeochemistry model, *Tellus*, 56B, 230-248, 2004.

1188 Feng, Z., Kobayashi, K., and Ainsworth, E. A.: Impact of elevated ozone concentration on growth,
1189 physiology, and yield of wheat (*Triticum aestivum* L.): a meta-analysis, *Global Change Biology*, 14,
1190 2696-2708, 10.1111/j.1365-2486.2008.01673.x, 2008.

1191 Fowler, D., Flechard, C., Cape, J. N., Storeton-West, R. L., and Coyle, M.: Measurements of Ozone
1192 Deposition to Vegetation Quantifying the Flux, the Stomatal and Non-Stomatal Components, *Water*,
1193 *Air, and Soil Pollution*, 130, 63-74, 10.1023/a:1012243317471, 2001.

1194 Fowler, D., Pilegaard, K., Sutton, M., Ambus, P., Raivonen, M., Duyzer, J., Simpson, D., Fagerli, H.,
1195 Fuzzi, S., and Schjørring, J. K.: Atmospheric composition change: ecosystems–atmosphere
1196 interactions, *Atmospheric Environment*, 43, 5193-5267, 2009.

1197 Franz, M., Simpson, D., Arneth, A., and Zaehle, S.: Development and evaluation of an ozone
1198 deposition scheme for coupling to a terrestrial biosphere model, *Biogeosciences*, 14, 45-71,
1199 doi:10.5194/bg-14-45-2017, 2017.

1200 Friedlingstein, P., Cox, P., Betts, R., Bopp, L., von Bloh, W., Brovkin, V., Cadule, P., Doney, S., Eby, M.,
1201 Fung, I., Bala, G., John, J., Jones, C., Joos, F., Kato, T., Kawamiya, M., Knorr, W., Lindsay, K.,
1202 Matthews, H. D., Raddatz, T., Rayner, P., Reick, C., Roeckner, E., Schnitzler, K. G., Schnur, R.,
1203 Strassmann, K., Weaver, A. J., Yoshikawa, C., and Zeng, N.: Climate–Carbon Cycle Feedback Analysis:
1204 Results from the C4MIP Model Intercomparison, *Journal of Climate*, 19, 3337-3353,
1205 10.1175/jcli3800.1, 2006.

1206 Fuentes, J. D., Wang, D., Bowling, D. R., Potosnak, M., Monson, R. K., Goliff, W. S., and Stockwell, W.
1207 R.: Biogenic hydrocarbon chemistry within and above a mixed deciduous forest, *Atmospheric*
1208 *Chemistry*, 56, 165-185, 2007.

1209 Fuhrer, J., Val Martin, M., Mills, G., Heald, C. L., Harmens, H., Hayes, F., Sharps, K., Bender, J., and
1210 Ashmore, M. R.: Current and future ozone risks to global terrestrial biodiversity and ecosystem
1211 processes, *Ecology and Evolution*, 6, 8785-8799, 10.1002/ece3.2568, 2016.

1212 Garland, J. A., and Derwent, R. G.: Destruction at the ground and the diurnal cycle of concentration
1213 of ozone and other gases, *Quarterly Journal of the Royal Meteorological Society*, 105, 169-183,
1214 doi:10.1002/qj.49710544311, 1979.

1215 Gedney, N., Cox, P. M., Bett, R. A., Boucher, O., Huntingford, C., and Stott, P. A.: Detection of a direct
1216 carbon dioxide effect in continental river runoff records, *Nature*, 439, 835-838, 2006.

1217 Gerosa, G., Marzuoli, R., Monteleone, B., Chiesa, M., and Finco, A.: Vertical Ozone Gradients above
1218 Forests. Comparison of Different Calculation Options with Direct Ozone Measurements above a
1219 Mature Forest and Consequences for Ozone Risk Assessment, *Forests*, 8, 337, 2017.

1220 Grantz, D., Gunn, S., and VU, H. B.: O₃ impacts on plant development: a meta-analysis of root/shoot
1221 allocation and growth, *Plant, cell & environment*, 29, 1193-1209, 2006.

1222 Harmens, H., Mills, G., Emberson, L. D., and Ashmore, M. R.: Implications of climate change for the
1223 stomatal flux of ozone: A case study for winter wheat, *Environmental Pollution*, 146, 763-770,
1224 <http://dx.doi.org/10.1016/j.envpol.2006.05.018>, 2007.

1225 Hayes, F., Wagg, S., Mills, G., Wilkinson, S., and Davies, W.: Ozone effects in a drier climate:
1226 implications for stomatal fluxes of reduced stomatal sensitivity to soil drying in a typical grassland
1227 species, *Global Change Biology*, 18, 948-959, 2012.

1228 Heikkinen, J., Ketoja, E., Nuutinen, V., and Regina, K.: Declining trend of carbon in Finnish cropland
1229 soils in 1974–2009, *Global Change Biology*, 19, 1456-1469, 10.1111/gcb.12137, 2013.

1230 Hofmockel, K. S., Zak, D. R., Moran, K. K., and Jastrow, J. D.: Changes in forest soil organic matter
1231 pools after a decade of elevated CO₂ and O₃, *Soil Biology and Biochemistry*, 43, 1518-1527,
1232 <http://dx.doi.org/10.1016/j.soilbio.2011.03.030>, 2011.

1233 Hoshika, Y., Watanabe, M., Inada, N., and Koike, T.: Ozone-induced stomatal sluggishness develops
1234 progressively in Siebold's beech (*Fagus crenata*), *Environmental Pollution*, 166, 152-156, 2012a.

1235 Hoshika, Y., Omasa, K., and Paoletti, E.: Whole-Tree Water Use Efficiency Is Decreased by Ambient
1236 Ozone and Not Affected by O₃-Induced Stomatal Sluggishness, *PLOS ONE*, 7, e39270,
1237 10.1371/journal.pone.0039270, 2012b.

1238 Hoshika, Y., Watanabe, M., Inada, N., and Koike, T.: Model-based analysis of avoidance of ozone
1239 stress by stomatal closure in Siebold's beech (*Fagus crenata*), *Annals of Botany*, 112, 1149-1158,
1240 2013.

1241 Hoshika, Y., Katata, G., Deushi, M., Watanabe, M., Koike, T., and Paoletti, E.: Ozone-induced stomatal
1242 sluggishness changes carbon and water balance of temperate deciduous forests., *Scientific Reports*,
1243 doi:10.1038/srep09871, 2015.

1244 Hurtt, G., Chini, L. P., Frolking, S., Betts, R., Feddema, J., Fischer, G., Fisk, J., Hibbard, K., Houghton,
1245 R., Janetos, A., and Jones, C. D.: Harmonization of land-use scenarios for the period 1500–2100: 600
1246 years of global gridded annual land-use transitions, wood harvest, and resulting secondary lands,
1247 *Climatic Change*, 109, 117-161, 2011.

1248 IGBP-DIS: International Geosphere-Biosphere Programme, Data and Information System, Potsdam,
1249 Germany. Available from Oak Ridge National Laboratory Distributed Active Archive Center, Oak
1250 Ridge, TN, available at: <http://www.daac.ornl.gov>,

1251 IPCC: Climate change 2013: The Physical Science Basis, IPCC Working Group I Contribution to AR5,
1252 2013.

1253 Jacobs, C. M. J.: Direct impact of atmospheric CO₂ enrichment on regional transpiration, Wageningen
1254 Agricultural University, 1994.

1255 Janssens, I. A., Freibauer, A., Ciais, P., Smith, P., Nabuurs, G.-J., Folberth, G., Schlamadinger, B.,
1256 Hutjes, R. W. A., Ceulemans, R., Schulze, E.-D., Valentini, R., and Dolman, A. J.: Europe's Terrestrial
1257 Biosphere Absorbs 7 to 12% of European Anthropogenic CO₂ Emissions, *Science*, 300, 1538-1542,
1258 10.1126/science.1083592, 2003.

1259 Jones, C. D., Cox, P., and Huntingford, C.: Uncertainty in climate–carbon-cycle projections associated
1260 with the sensitivity of soil respiration to temperature, *Tellus B*, 55, 642-648, 10.1034/j.1600-
1261 0889.2003.01440.x, 2003.

1262 Jung, M., Reichstein, M., Margolis, H. A., Cescatti, A., Richardson, A. D., Arain, M. A., Arneth, A.,
1263 Bernhofer, C., Bonal, D., Chen, J., Gianelle, D., Gobron, N., Kiely, G., Kutsch, W., Lasslop, G., Law, B.
1264 E., Lindroth, A., Merbold, L., Montagnani, L., Moors, E. J., Papale, D., Sottocornola, M., Vaccari, F.,
1265 and Williams, C.: Global patterns of land-atmosphere fluxes of carbon dioxide, latent heat, and
1266 sensible heat derived from eddy covariance, satellite, and meteorological observations, *Journal of*
1267 *Geophysical Research: Biogeosciences*, 116, n/a-n/a, 10.1029/2010JG001566, 2011.

1268 Kala, J., De Kauwe, M. G., Pitman, A. J., Medlyn, B. E., Wang, Y. P., Lorenz, R., and Perkins-Kirkpatrick,
1269 S. E.: Impact of the representation of stomatal conductance on model projections of heatwave
1270 intensity., *Scientific Reports*, 1-7, 10.1038/srep23418, 2016.

1271 Karlsson, P., Hansson, M., Höglund, H. O., and Pleijel, H.: Ozone concentration gradients and wind
1272 conditions in Norway spruce (*Picea abies*) forests in Sweden, *Atmospheric Environment*, 1610-1618
1273 pp., 2006.

1274 Karlsson, P. E., Braun, S., Broadmeadow, M., Elvira, S., Emberson, L., Gimeno, B. S., Le Thiec, D.,
1275 Novak, K., Oksanen, E., Schaub, M., Uddling, J., and Wilkinson, M.: Risk assessments for forest trees:
1276 The performance of the ozone flux versus the AOT concepts, *Environmental Pollution*, 146, 608-616,
1277 <http://dx.doi.org/10.1016/j.envpol.2006.06.012>, 2007.

1278 Karnosky, D., Percy, K. E., Xiang, B., Callan, B., Noormets, A., Mankovska, B., Hopkin, A., Sober, J.,
1279 Jones, W., and Dickson, R.: Interacting elevated CO₂ and tropospheric O₃ predisposes aspen
1280 (*Populus tremuloides* Michx.) to infection by rust (*Melampsora medusae* f. sp. *tremuloidae*), *Global*
1281 *Change Biology*, 8, 329-338, 2002.

1282 Karnosky, D. F., Skelly, J. M., Percy, K. E., and Chappelka, A. H.: Perspectives regarding 50years of
1283 research on effects of tropospheric ozone air pollution on US forests, *Environmental Pollution*, 147,
1284 489-506, 2007.

1285 Keeling, C. D., and Whorf, T. P.: Atmospheric CO₂ records from sites in the SIO air sampling network.
1286 In *Trends: A Compendium of Data on Global Change*, Carbon Dioxide Information Analysis Center,
1287 Oak Ridge National Laboratory, Oak Ridge, Tenn., U.S.A. , 2004.

1288 Kitao, M., Löw, M., Heerdt, C., Grams, T. E., Häberle, K.-H., and Matyssek, R.: Effects of chronic
1289 elevated ozone exposure on gas exchange responses of adult beech trees (*Fagus sylvatica*) as related
1290 to the within-canopy light gradient, *Environmental Pollution*, 157, 537-544, 2009.

1291 Kjellström, E., Nikulin, G., Hansson, U., Strandberg, G., and Ullerstig, A.: 21st century changes in the
1292 European climate: uncertainties derived from an ensemble of regional climate model simulations,
1293 *Tellus A*, 63, 24-40, 2011.

1294 Kubiske, M., Quinn, V., Marquardt, P., and Karnosky, D.: Effects of Elevated Atmospheric CO₂ and/or
1295 O₃ on Intra-and Interspecific Competitive Ability of Aspen, *Plant biology*, 9, 342-355, 2007.

1296 Lamarque, J., Shindell, D. T., Josse, B., Young, P., Cionni, I., Eyring, V., Bergmann, D., Cameron-Smith,
1297 P., Collins, W. J., and Doherty, R.: The Atmospheric Chemistry and Climate Model Intercomparison
1298 Project (ACCMIP): overview and description of models, simulations and climate diagnostics,
1299 *Geoscientific Model Development*, 6, 179-206, 2013.

1300 Langner, J., Engardt, M., Baklanov, A., Christensen, J. H., Gauss, M., Geels, C., Hedegaard, G. B.,
1301 Nuterman, R., Simpson, D., and Soares, J.: A multi-model study of impacts of climate change on
1302 surface ozone in Europe, *Atmospheric Chemistry and Physics*, 12, 10423-10440, 2012a.

1303 Langner, J., Engardt, M., and Andersson, C.: European summer surface ozone 1990–2100,
1304 *Atmospheric Chemistry and Physics*, 12, 10097-10105, 2012b.

1305 Le Quéré, C., Moriarty, R., Andrew, R. M., Peters, G. P., Ciais, P., Friedlingstein, P., Jones, S. D., Sitch,
1306 S., Tans, P., Arneth, A., Boden, T. A., Bopp, L., Bozec, Y., Canadell, J. G., Chini, L. P., Chevallier, F.,
1307 Cosca, C. E., Harris, I., Hoppema, M., Houghton, R. A., House, J. I., Jain, A. K., Johannessen, T., Kato,
1308 E., Keeling, R. F., Kitidis, V., Klein Goldewijk, K., Koven, C., Landa, C. S., Landschützer, P., Lenton, A.,
1309 Lima, I. D., Marland, G., Mathis, J. T., Metzl, N., Nojiri, Y., Olsen, A., Ono, T., Peng, S., Peters, W., Pfeil,

1310 B., Poulter, B., Raupach, M. R., Regnier, P., Rödenbeck, C., Saito, S., Salisbury, J. E., Schuster, U.,
1311 Schwinger, J., Séférian, R., Segschneider, J., Steinhoff, T., Stocker, B. D., Sutton, A. J., Takahashi, T.,
1312 Tilbrook, B., van der Werf, G. R., Viovy, N., Wang, Y. P., Wanninkhof, R., Wiltshire, A., and Zeng, N.:
1313 Global carbon budget 2014, *Earth Syst. Sci. Data*, 7, 47-85, 10.5194/essd-7-47-2015, 2015.

1314 Le Quéré, C., Andrew, R. M., Canadell, J. G., Sitch, S., Korsbakken, J. I., Peters, G. P., Manning, A. C.,
1315 Boden, T. A., Tans, P. P., Houghton, R. A., Keeling, R. F., Alin, S., Andrews, O. D., Anthoni, P., Barbero,
1316 L., Bopp, L., Chevallier, F., Chini, L. P., Ciais, P., Currie, K., Delire, C., Doney, S. C., Friedlingstein, P.,
1317 Gkritzalis, T., Harris, I., Hauck, J., Haverd, V., Hoppema, M., Klein Goldewijk, K., Jain, A. K., Kato, E.,
1318 Körtzinger, A., Landschützer, P., Lefèvre, N., Lenton, A., Lienert, S., Lombardozzi, D., Melton, J. R.,
1319 Metzl, N., Millero, F., Monteiro, P. M. S., Munro, D. R., Nabel, J. E. M. S., Nakaoka, S. I., O'Brien, K.,
1320 Olsen, A., Omar, A. M., Ono, T., Pierrot, D., Poulter, B., Rödenbeck, C., Salisbury, J., Schuster, U.,
1321 Schwinger, J., Séférian, R., Skjelvan, I., Stocker, B. D., Sutton, A. J., Takahashi, T., Tian, H., Tilbrook, B.,
1322 van der Laan-Luijkx, I. T., van der Werf, G. R., Viovy, N., Walker, A. P., Wiltshire, A. J., and Zaehle, S.:
1323 Global Carbon Budget 2016, *Earth Syst. Sci. Data*, 8, 605-649, 10.5194/essd-8-605-2016, 2016.

1324 Le Quéré, C., Andrew, R. M., Friedlingstein, P., Sitch, S., Pongratz, J., Manning, A. C., Korsbakken, J. I.,
1325 Peters, G. P., Canadell, J. G., Jackson, R. B., Boden, T. A., Tans, P. P., Andrews, O. D., Arora, V. K.,
1326 Bakker, D. C. E., Barbero, L., Becker, M., Betts, R. A., Bopp, L., Chevallier, F., Chini, L. P., Ciais, P.,
1327 Cosca, C. E., Cross, J., Currie, K., Gasser, T., Harris, I., Hauck, J., Haverd, V., Houghton, R. A., Hunt, C.
1328 W., Hurtt, G., Ilyina, T., Jain, A. K., Kato, E., Kautz, M., Keeling, R. F., Klein Goldewijk, K., Körtzinger,
1329 A., Landschützer, P., Lefèvre, N., Lenton, A., Lienert, S., Lima, I., Lombardozzi, D., Metzl, N., Millero,
1330 F., Monteiro, P. M. S., Munro, D. R., Nabel, J. E. M. S., Nakaoka, S.-I., Nojiri, Y., Padín, X. A., Pregon,
1331 A., Pfeil, B., Pierrot, D., Poulter, B., Rehder, G., Reimer, J., Rödenbeck, C., Schwinger, J., Séférian, R.,
1332 Skjelvan, I., Stocker, B. D., Tian, H., Tilbrook, B., van der Laan-Luijkx, I. T., van der Werf, G. R., van
1333 Heuven, S., Viovy, N., Vuichard, N., Walker, A. P., Watson, A. J., Wiltshire, A. J., Zaehle, S., and Zhu,
1334 D.: Global Carbon Budget 2017, *Earth Syst. Sci. Data Discuss*, in review, 2017.

1335 Leuzinger, S., and Körner, C.: Water savings in mature deciduous forest trees under elevated CO₂,
1336 *Global Change Biology*, 13, 2498-2508, doi:10.1111/j.1365-2486.2007.01467.x, 2007.

1337 Lin, Y.-S., Medlyn, B. E., Duursma, R. A., Prentice, I. C., Wang, H., Baig, S., Eamus, D., de Dios, V. R.,
1338 Mitchell, P., and Ellsworth, D. S.: Optimal stomatal behaviour around the world, *Nature Climate*
1339 *Change*, 5, 459-464, 2015.

1340 Lindroth, R. L.: Impacts of Elevated Atmospheric CO₂ and O₃ on Forests: Phytochemistry, Trophic
1341 Interactions, and Ecosystem Dynamics, *Journal of Chemical Ecology*, 36, 2-21, 10.1007/s10886-009-
1342 9731-4, 2010.

1343 Logan, J. A., Staehelin, J., Megretskaia, I. A., Cammas, J. P., Thouret, V., Claude, H., De Backer, H.,
1344 Steinbacher, M., Scheel, H. E., Stübi, R., Fröhlich, M., and Derwent, R.: Changes in ozone over
1345 Europe: Analysis of ozone measurements from sondes, regular aircraft (MOZAIC) and alpine surface
1346 sites, *Journal of Geophysical Research*, 117, 1-23, 2012.

1347 Lombardozzi, D., Levis, S., Bonan, G., and Sparks, J. P.: Predicting photosynthesis and transpiration
1348 responses to ozone: decoupling modeled photosynthesis and stomatal conductance, *Biogeosciences*,
1349 3113-3130, 2012.

1350 Lombardozzi, D., Levis, S., Bonan, G., Hess, P. G., and Sparks, J. P.: The Influence of Chronic Ozone
1351 Exposure on Global Carbon and Water Cycles, *Journal of Climate*, 28, 292-305, 10.1175/jcli-d-14-
1352 00223.1, 2015.

1353 Long, S. P., Ainsworth, E. A., Leakey, A. D. B., Nosberger, J., and Ort, D. R.: Food for Thought: Lower-
1354 Than-Expected Crop Yield Stimulation with Rising CO₂ Concentrations, *Science*, 312, 1918-1921,
1355 10.1126/science.1114722, 2006.

1356 Löw, M., Herbinger, K., Nunn, A., Häberle, K.-H., Leuchner, M., Heerdt, C., Werner, H., Wipfler, P.,
1357 Pretzsch, H., and Tausz, M.: Extraordinary drought of 2003 overrules ozone impact on adult beech
1358 trees (*Fagus sylvatica*), *Trees*, 20, 539-548, 2006.

1359 Loya, W. M., Pregitzer, K. S., Karberg, N. J., King, J. S., and Giardina, C. P.: Reduction of soil carbon
1360 formation by tropospheric ozone under increased carbon dioxide levels., *Nature*, 425, 705-707,
1361 2003.

1362 Luyssaert, S., Abril, G., Andres, R., Bastviken, D., Bellassen, V., Bergamaschi, P., Bousquet, P.,
1363 Chevallier, F., Ciais, P., Corazza, M., Dechow, R., Erb, K. H., Etiope, G., Fortems-Cheiney, A., Grassi, G.,
1364 Hartmann, J., Jung, M., Lathière, J., Lohila, A., Mayorga, E., Moosdorf, N., Njakou, D. S., Otto, J.,
1365 Papale, D., Peters, W., Peylin, P., Raymond, P., Rödenbeck, C., Saarnio, S., Schulze, E. D., Szopa, S.,
1366 Thompson, R., Verkerk, P. J., Vuichard, N., Wang, R., Wattenbach, M., and Zaehle, S.: The European
1367 land and inland water CO₂, CO, CH₄ and N₂O balance between 2001 and 2005, *Biogeosciences*, 9,
1368 3357-3380, 10.5194/bg-9-3357-2012, 2012.

1369 Massman, W. J.: A review of the molecular diffusivities of H₂O, CO₂, CH₄, CO, O₃, SO₂, NH₃, N₂O,
1370 NO, and NO₂ in air, O₂ and N₂ near STP, *Atmospheric Environment*, 32, 1111-1127,
1371 [http://dx.doi.org/10.1016/S1352-2310\(97\)00391-9](http://dx.doi.org/10.1016/S1352-2310(97)00391-9), 1998.

1372 Matussek, R., Wieser, G., Ceulemans, R., Rennenberg, H., Pretzsch, H., Haberer, K., Löw, M., Nunn,
1373 A., Werner, H., and Wipfler, P.: Enhanced ozone strongly reduces carbon sink strength of adult beech
1374 (*Fagus sylvatica*)—Resume from the free-air fumigation study at Kranzberg Forest, *Environmental*
1375 *Pollution*, 158, 2527-2532, 2010a.

1376 Matussek, R., Karnosky, D., Wieser, G., Percy, K., Oksanen, E., Grams, T., Kubiske, M., Hanke, D., and
1377 Pretzsch, H.: Advances in understanding ozone impact on forest trees: messages from novel
1378 phytotron and free-air fumigation studies, *Environmental Pollution*, 158, 1990-2006, 2010b.

1379 McLaughlin, S. B., Nosal, M., Wullschlegel, S. D., and Sun, G.: Interactive effects of ozone and climate
1380 on tree growth and water use in a southern Appalachian forest in the USA, *New Phytologist*, 174,
1381 109-124, 10.1111/j.1469-8137.2007.02018.x, 2007a.

1382 McLaughlin, S. B., Wullschlegel, S. D., Sun, G., and Nosal, M.: Interactive effects of ozone and climate
1383 on water use, soil moisture content and streamflow in a southern Appalachian forest in the USA,
1384 *New Phytologist*, 174, 125-136, 10.1111/j.1469-8137.2007.01970.x, 2007b.

1385 Medlyn, B. E., Badeck, F. W., De Pury, D. G. G., Barton, C. V. M., Broadmeadow, M., Ceulemans, R.,
1386 De Angelis, P., Forstreuter, M., Jach, M. E., Kellomaki, S., Laitat, E., Marek, M., Philippot, S., Rey, A.,
1387 Strassmeyer, J., Laitinen, K., Liozon, R., Portier, B., Roberntz, P., Wang, K., and Jstbid, P. G.: Effects
1388 of elevated [CO₂] on photosynthesis in European forest species: a meta-analysis of model
1389 parameters, *Plant, Cell & Environment*, 22, 1475-1495, doi:10.1046/j.1365-3040.1999.00523.x, 1999.

1390 Medlyn, B. E., Barton, C. V. M., Broadmeadow, M. S. J., Ceulemans, R., De Angelis, P., Forstreuter,
1391 M., Freeman, M., Jackson, S. B., Kellomaki, S., Laitat, E., Rey, A., Roberntz, P., Sigurdsson, B. D.,
1392 Strassmeyer, J., Wang, K., Curtis, P. S., and Jarvis, P. G.: Stomatal conductance of forest species
1393 after long-term exposure to elevated CO₂ concentration: a synthesis, *New Phytologist*, 149, 247-264,
1394 2001.

1395 Medlyn, B. E., Duursma, R. A., Eamus, D., Ellsworth, D. S., Prentice, I. C., Barton, C. V., Crous, K. Y., de
1396 Angelis, P., Freeman, M., and Wingate, L.: Reconciling the optimal and empirical approaches to
1397 modelling stomatal conductance, *Global Change Biology*, 17, 2134-2144, 2011.

1398 Mercado, L. M., Bellouin, N., Sitch, S., Boucher, O., Huntingford, C., Wild, M., and Cox, P. M.: Impact
1399 of changes in diffuse radiation on the global land carbon sink, *Nature*, 458, 1014-1017,
1400 http://www.nature.com/nature/journal/v458/n7241/supinfo/nature07949_S1.html, 2009.

1401 Mills, G., Hayes, F., Wilkinson, S., and Davies, W. J.: Chronic exposure to increasing background
1402 ozone impairs stomatal functioning in grassland species, *Global Change Biology*, 15, 1522-1533,
1403 2009.

1404 Mills, G., Pleijel, H., Braun, S., Büker, P., Bermejo, V., Calvo, E., Danielsson, H., Emberson, L.,
1405 Grünhage, L., Fernández, I. G., Harmens, H., Hayes, F., Karlsson, P.-E., and Simpson, D.: New stomatal
1406 flux-based critical levels for ozone effects on vegetation, *Atmospheric Environment*, 5064-5068,
1407 2011a.

1408 Mills, G., Hayes, F., Simpson, D., Emberson, L., Norris, D., Harmens, H., and BÜKER, P.: Evidence of
1409 widespread effects of ozone on crops and (semi-)natural vegetation in Europe (1990–2006) in

1410 relation to AOT40- and flux-based risk maps, *Global Change Biology*, 17, 592-613, 10.1111/j.1365-
1411 2486.2010.02217.x, 2011b.

1412 Mills, G., Harmens, H., Wagg, S., Sharps, K., Hayes, F., Fowler, D., Sutton, M., and Davies, B.: Ozone
1413 impacts on vegetation in a nitrogen enriched and changing climate, *Environmental Pollution*, 208,
1414 898-908, 2016.

1415 Norby, R. J., Wullschleger, S. D., Gunderson, C. A., Johnson, D. W., and Ceulemans, R.: Tree responses
1416 to rising CO₂ in field experiments: implications for the future forest, *Plant, Cell and Environment*, 22,
1417 683-714, 1999.

1418 Norby, R. J., DeLucia, E. H., Gielen, B., Calfapietra, C., Giardina, C. P., King, J. S., Ledford, J., McCarthy,
1419 H. R., Moore, D. J. P., Ceulemans, R., De Angelis, P., Finzi, A. C., Karnosky, D. F., Kubiske, M. E., Lukac,
1420 M., Pregitzer, K. S., Scarascia-Mugnozza, G. E., Schlesinger, W. H., and Oren, R.: Forest response to
1421 elevated CO₂ is conserved across a broad range of productivity, *Proc. Natl. Acad. Sci. U. S. A.*, 102,
1422 18052-18056, 10.1073/pnas.0509478102, 2005.

1423 Nunn, A. J., Reiter, I. M., Häberle, K.-H., Langebartels, C., Bahnweg, G., Pretzsch, H., Sandermann, H.,
1424 and Matyssek, R.: Response patterns in adult forest trees to chronic ozone stress: identification of
1425 variations and consistencies, *Environmental Pollution*, 136, 365-369, 2005.

1426 O'Connor, F. M., Johnson, C. E., Morgenstern, O., Abraham, N. L., Braesicke, P., Dalvi, M., Folberth,
1427 G. A., Sanderson, M. G., Telford, P. J., Voulgarakis, A., Young, P. J., Zeng, G., Collins, W. J., and Pyle, J.
1428 A.: Evaluation of the new UKCA climate-composition model – Part 2: The Troposphere, *Geosci.
1429 Model Dev.*, 7, 41-91, 10.5194/gmd-7-41-2014, 2014.

1430 Paoletti, E., and Grulke, N. E.: Ozone exposure and stomatal sluggishness in different plant
1431 physiognomic classes, *Environmental Pollution*, 158, 2664-2671, 2010.

1432 Parrish, D. D., Law, K. S., Staehelin, J., Derwent, R., Cooper, O. R., Tanimoto, H., Volz-Thomas, A.,
1433 Gilge, S., Scheel, H. E., Steinbacher, M., and Chan, E.: Long-term changes in lower tropospheric
1434 baseline ozone concentrations at northern mid-latitudes, *Atmos. Chem. Phys.*, 12, 11485-11504,
1435 10.5194/acp-12-11485-2012, 2012.

1436 Parrish, D. D., Law, K. S., Staehelin, J., Derwent, R., Cooper, O. R., Tanimoto, H., Volz-Thomas, A.,
1437 Gilge, S., Scheel, H. E., Steinbacher, M., and Chan, E.: Lower tropospheric ozone at northern
1438 midlatitudes: Changing seasonal cycle, *Geophysical Research Letters*, 40, 1631-1636, 2013.

1439 Percy, K. E., Awmack, C. S., Lindroth, R. L., Kubiske, M. E., Kopper, B. J., Isebrands, J., Pregitzer, K. S.,
1440 Hendrey, G. R., Dickson, R. E., and Zak, D. R.: Altered performance of forest pests under atmospheres
1441 enriched by CO₂ and O₃, *Nature*, 420, 403-407, 2002.

1442 Royal-Society: Ground-level ozone in the 21st century: future trends, impacts and policy
1443 implications, *Science Policy Report 15/08*, 2008.

1444 Samuelsson, P., Jones, C. G., Willén, U., Ullerstig, A., Gollvik, S., Hansson, U., Jansson, C., Kjellström,
1445 E., Nikulin, G., and Wyser, K.: The Rossby Centre Regional Climate model RCA3: model description
1446 and performance, *Tellus A*, 63, 4-23, 2011.

1447 Saxe, H., Ellsworth, D. S., and Heath, J.: Tree and forest functioning in an enriched CO₂ atmosphere,
1448 *New Phytologist*, 139, 395-436, doi:10.1046/j.1469-8137.1998.00221.x, 1998.

1449 Schulze, E.-D., Ciais, P., Luyssaert, S., Schruppf, M., Janssens, I. A., Thiruchittampalam, B., Theloke, J.,
1450 Saurat, M., Bringezu, S., and Lelieveld, J.: The European carbon balance. Part 4: integration of carbon
1451 and other trace-gas fluxes, *Global Change Biology*, 16, 1451-1469, 2010.

1452 Schulze, E. D., Luyssaert, S., Ciais, P., Freibauer, A., Janssens, I. A., and et al.: Importance of methane
1453 and nitrous oxide for Europe's terrestrial greenhouse-gas balance, *Nature Geosci*, 2, 842-850,
1454 http://www.nature.com/ngeo/journal/v2/n12/supinfo/ngeo686_S1.html, 2009.

1455 Sicard, P., De Marco, A., Troussier, F., Renoua, C., Vas, N., and Paoletti, E.: Decrease in surface ozone
1456 concentrations at Mediterranean remote sites and increase in the cities, *Atmospheric Environment*,
1457 79, 705-715, 2013.

1458 Simpson, D., Emberson, L., Ashmore, M., and Tuovinen, J.: A comparison of two different approaches
1459 for mapping potential ozone damage to vegetation. A model study *Environmental Pollution*, 146,
1460 715-725, 2007.

1461 Simpson, D., Benedictow, A., Berge, H., Bergström, R., Emberson, L. D., Fagerli, H., Flechard, C. R.,
1462 Hayman, G. D., Gauss, M., and Jonson, J. E.: The EMEP MSC-W chemical transport model—technical
1463 description, *Atmospheric Chemistry and Physics*, 12, 7825-7865, 2012.

1464 Simpson, D., Andersson, C., Christensen, J. H., Engardt, M., Geels, C., Nyiri, A., Posch, M., Soares, J.,
1465 Sofiev, M., and Wind, P.: Impacts of climate and emission changes on nitrogen deposition in Europe:
1466 a multi-model study, *Atmospheric Chemistry and Physics*, 14, 6995-7017, 2014a.

1467 Simpson, D., Arneth, A., Mills, G., Solberg, S., and Uddling, J.: Ozone—the persistent menace:
1468 interactions with the N cycle and climate change, *Current Opinion in Environmental Sustainability*, 9,
1469 9-19, 2014b.

1470 Sitch, S., Cox, P. M., Collins, W. J., and Huntingford, C.: Indirect radiative forcing of climate change
1471 through ozone effects on the land-carbon sink, *Nature*, 448, 791-794,
1472 http://www.nature.com/nature/journal/v448/n7155/supinfo/nature06059_S1.html, 2007.

1473 Sitch, S., Friedlingstein, P., Gruber, N., Jones, S. D., Murray-Tortarolo, G., Ahlström, A., Doney, S. C.,
1474 Graven, H., Heinze, C., Huntingford, C., Levis, S., Levy, P. E., Lomas, M., Poulter, B., Viovy, N., Zaehle,
1475 S., Zeng, N., Arneth, A., Bonan, G., Bopp, L., Canadell, J. G., Chevallier, F., Ciais, P., Ellis, R., Gloor, M.,
1476 Peylin, P., Piao, S. L., Le Quéré, C., Smith, B., Zhu, Z., and Myneni, R.: Recent trends and drivers of
1477 regional sources and sinks of carbon dioxide, *Biogeosciences*, 12, 653-679, 10.5194/bg-12-653-2015,
1478 2015.

1479 Sleutel, S., De Neve, S., and Hofman, G.: Estimates of carbon stock changes in Belgian cropland., *Soil*
1480 *Use and Management*, 19, 166-171, 10.1079/SUM2003187, 2003.

1481 Sun, G. E., McLaughlin, S. B., Porter, J. H., Uddling, J., Mulholland, P. J., Adams, M. B., and Pederson,
1482 N.: Interactive influences of ozone and climate on streamflow of forested watersheds, *Global Change*
1483 *Biology*, 18, 3395-3409, 10.1111/j.1365-2486.2012.02787.x, 2012.

1484 Tai, P. K. A., Val Martin, M., and Heald, C. L.: Threat to future global food security from climate
1485 change and ozone air pollution, *Nature Climate Change*, 4, 817 - 821, 2014.

1486 Talhelm, A. F., Pregitzer, K. S., Kubiske, M. E., Zak, D. R., Company, C. E., Burton, A. J., Dickson, R. E.,
1487 Hendrey, G. R., Isebrands, J. G., Lewin, K. F., Nagy, J., and Karnosky, D. F.: Elevated carbon dioxide
1488 and ozone alter productivity and ecosystem carbon content in northern temperate forests, *Global*
1489 *Change Biology*, 20, 2492-2504, 10.1111/gcb.12564, 2014.

1490 Tans, P., and Keeling, R.: Dr. Pieter Tans, NOAA/ESRL (www.esrl.noaa.gov/gmd/ccgg/trends/) and Dr.
1491 Ralph Keeling, Scripps Institution of Oceanography (scrippsco2.ucsd.edu/).

1492 Tans, P., and Keeling, R.: NOAA/ESRL (www.esrl.noaa.gov/gmd/ccgg/trends/), Scripps Institution of
1493 Oceanography (scrippsco2.ucsd.edu/). , 2014.

1494 Tricker, P. J., Pecchiari, M., Bunn, S. M., Vaccari, F. P., Peressotti, A., Miglietta, F., and Taylor, G.:
1495 Water use of a bioenergy plantation increases in a future high CO₂ world, *Biomass and Bioenergy*,
1496 33, 200-208, 2009.

1497 Tuovinen, J.-P., Emberson, L., and Simpson, D.: Modelling ozone fluxes to forests for risk assessment:
1498 status and prospects, *Annals of Forest Science*, 66, 1-14, 2009.

1499 Tuovinen, J., Hakola, H., Karlsson, P., and Simpson, D.: Air pollution risks to Northern European
1500 forests in a changing climate, *Climate Change, Air Pollution and Global Challenges Understanding*
1501 *and Perspectives from Forest Research*, 2013.

1502 Uddling, J., Teclaw, R. M., Pregitzer, K. S., and Ellsworth, D. S.: Leaf and canopy conductance in aspen
1503 and aspen-birch forests under free-air enrichment of carbon dioxide and ozone, *Tree Physiology*, 29,
1504 1367-1380, 2009.

1505 Val Martin, M., Heald, C. L., and Arnold, S. R.: Coupling dry deposition to vegetation phenology in the
1506 Community Earth System Model: Implications for the simulation of surface O₃, *Geophysical*
1507 *Research Letters*, 41, 2988-2996, doi:10.1002/2014GL059651, 2014.

1508 van Vuuren, D. P., Edmonds, J., Kainuma, M., Riahi, K., Thomson, A., Hibbard, K., Hurtt, G. C., Kram,
1509 T., Krey, V., Lamarque, J.-F., Masui, T., Meinshausen, M., Nakicenovic, N., Smith, S. J., and Rose, S. K.:
1510 The representative concentration pathways: an overview, *Climatic Change*, 109, 5, 10.1007/s10584-
1511 011-0148-z, 2011.

1512 Verstraeten, W. W., Neu, J. L., Williams, J. E., Bowman, K. W., Worden, J. R., and Boersma, K. F.:
1513 Rapid increases in tropospheric ozone production and export from China, *Nature Geoscience* 8, 690-
1514 695, 2015.

1515 Vingarzan, R.: A review of surface ozone background levels and trends, *Atmospheric Environment*,
1516 38, 3431-3442, <https://doi.org/10.1016/j.atmosenv.2004.03.030>, 2004.

1517 Weedon, G. P., Gomes, S., Viterbo, P., Österle, H., Adam, J. C., Bellouin, N., Boucher, O., and Best, M.
1518 J.: The WATCH Forcing Data 1958-2001: a meteorological forcing dataset for land surface- and
1519 hydrological models. , WATCH Tech. Rep. 22, 41p (available at www.eu-watch.org/publications).
1520 2010.

1521 Weedon, G. P., Gomes, S., Viterbo, P., Shuttleworth, W. J., Blyth, E., Österle, H., Adam, J. C., Bellouin,
1522 N., Boucher, O., and Best, M.: Creation of the WATCH Forcing data and its use to assess global and
1523 regional reference crop evaporation over land during the twentieth century, *Journal of*
1524 *Hydrometeorology*, 12, 823-848, doi: 10.1175/2011JHM1369.1., 2011.

1525 Weedon, G. P.: Readme file for the "WFDEI" dataset.available at: [http://www.eu-](http://www.eu-watch.org/gfx_content/documents/README-WFDEI.pdf)
1526 [watch.org/gfx_content/documents/README-WFDEI.pdf](http://www.eu-watch.org/gfx_content/documents/README-WFDEI.pdf), 2013.

1527 Wild, O.: Modelling the global tropospheric ozone budget: exploring the
1528 variability in current models, *Atmospheric Chemistry and Physics*, 2643–2660, 2007.

1529 Wilkinson, S., and Davies, W. J.: Ozone suppresses soil drying-and abscisic acid (ABA)-induced
1530 stomatal closure via an ethylene-dependent mechanism, *Plant, Cell & Environment*, 32, 949-959,
1531 2009.

1532 Wilkinson, S., and Davies, W. J.: Drought, ozone, ABA and ethylene: new insights from cell to plant to
1533 community, *Plant, Cell & Environment*, 33, 510-525, 10.1111/j.1365-3040.2009.02052.x, 2010.

1534 Wittig, V. E., Ainsworth, E. A., and Long, S. P.: To what extent do current and projected increases in
1535 surface ozone affect photosynthesis and stomatal conductance of trees? A meta-analytic review of
1536 the last 3 decades of experiments, *Plant, Cell & Environment*, 30, 1150-1162, 10.1111/j.1365-
1537 3040.2007.01717.x, 2007.

1538 Wittig, V. E., Ainsworth, E. A., Naidu, S. L., Karnosky, D. F., and Long, S. P.: Quantifying the impact of
1539 current and future tropospheric ozone on tree biomass, growth, physiology and biochemistry: a
1540 quantitative meta-analysis, *Global Change Biology*, 15, 396-424, 10.1111/j.1365-2486.2008.01774.x,
1541 2009.

1542 Wullschleger, S. D., Gunderson, C. A., Hanson, P. J., Wilson, K. B., and Norby, R. J.: Sensitivity of
1543 stomatal and canopy conductance to elevated CO₂ concentration; interacting variables and
1544 perspectives of scale, *New Phytologist*, 153, 485-496, doi:10.1046/j.0028-646X.2001.00333.x, 2002.

1545 Young, P., Arneth, A., Schurgers, G., Zeng, G., and Pyle, J. A.: The CO₂ inhibition of terrestrial isoprene
1546 emission significantly affects future ozone projections, *Atmospheric Chemistry and Physics*, 9, 2793-
1547 2803, 2009.

1548 Young, P., Archibald, A., Bowman, K., Lamarque, J.-F., Naik, V., Stevenson, D., Tilmes, S., Voulgarakis,
1549 A., Wild, O., and Bergmann, D.: Pre-industrial to end 21st century projections of tropospheric ozone
1550 from the Atmospheric Chemistry and Climate Model Intercomparison Project (ACCMIP),
1551 *Atmospheric Chemistry and Physics*, 13, 2063-2090, 2013.

1552 Zaehle, S.: Terrestrial nitrogen–carbon cycle interactions at the global scale, *Philosophical*
1553 *Transactions of the Royal Society B: Biological Sciences*, 368, 20130125, 10.1098/rstb.2013.0125,
1554 2013.

1555 Zak, D. R., Pregitzer, K. S., Kubiske, M. E., and Burton, A. J.: Forest productivity under elevated CO₂
1556 and O₃: positive feedbacks to soil N cycling sustain decade-long net primary productivity
1557 enhancement by CO₂, *Ecology Letters*, 14, 1220-1226, 10.1111/j.1461-0248.2011.01692.x, 2011.

1558

1559

1560

1561

1562 Response to Reviewers comments

1563

1564 We would like to thank the reviewer again for their time to read the manuscript and comment on it. This has
1565 improved the manuscript and we hope the reviewer finds our changes satisfactory. Please find our comments
1566 below.

1567

1568 Thanks to the authors for moving the discussion of the calibration to the main text. I think this
1569 strengthens the paper, and clarifies the novelty of the work. I think the work should be
1570 published after the authors address minor revisions.

1571

1572 General comments.

1573 I don't find the naming of the different simulations to O₃, CO₂, and CO₂+O₃ very helpful
1574 especially when the authors are referring to the gases as O₃ and CO₂ at the same time.
1575 Something like run_O₃, or run_CO₂, run_both_O₃_CO₂?

1576

1577 We have renamed the simulations as advised above.

1578

1579 I'm a bit confused with respect to the title of the paper, especially because the authors have
1580 a
1581 section dedicated to their findings that the impact isn't as large as expected.

1582

1583 The title reflects that our simulations show a large impact of O₃ from 1901 to present day, but this decreases
1584 significantly into the future.

1585

1586 Line-by-line comments.

1587 Lines 39: "its interaction with CO₂" does not sit well with me because CO₂ and O₃ are not
1588 directly interacting — rather there are interactive effects of CO₂ and O₃. Please revise.

1589

1590 This has been amended (Line 39):

1591

1592 "We conduct our analysis specifically for the European region to quantify the impact of the interactive effects of
1593 tropospheric O₃ and CO₂ on gross primary productivity (GPP) and land carbon storage across Europe."

1594

1595 Lines 44-46: At this point in the abstract the readers don't know what high and low sensitivity
1596 are

1597

1598 This has been amended (Line 45-46):

1599

1600 "This alleviation of O₃ damage by CO₂ induced stomatal closure was around 1 to 2% for both land carbon and
1601 GPP, depending on plant sensitivity to O₃."

1602

1603 Line 62: citation should be parenthetical

1604

1605 This has been changed.

1606

1607 Line 86: authors should define what they mean by background ozone

1608

1609 We define background ozone (Line88-89):

1610

1611 "Background O₃ is generally defined as the O₃ pollution present in a region that is not attributed to local
1612 anthropogenic sources (Vingarzan, 2004)."

1613

1614 Line 94: "long-range transport of ozone"

1615

1616 This has been changed (Line 96).

1617

1618 Line 100: why are there two “e.g.”s? What is Sicard et al. (2013) a reference here for?
1619
1620 This has been changed (Line 102).
1621
1622 Line 103: I would suggest cutting “currently have poor emission controls”
1623
1624 This has been removed (Line 105).
1625
1626 Line 108-109: Is there a lot of transport of ozone into Europe? I think references are needed
1627 here, or this line should be cut.
1628
1629 Two references were added here (Line 111):
1630
1631 (Auvray and Bey, 2005;Derwent et al., 2015)
1632
1633 Line 112-113: Having this statement here could be misleading — for example, if a reader
1634 thought the impact of ozone on vegetation was through it’s ability to trap heat. It would be
1635 more clear if after “direct radiative forcing of ozone”, the authors added “, a potent
1636 greenhouse
1637 gas, ”
1638 This sentence has been removed, and suggested changes made (Line 113 to 120):
1639
1640 “Rising background O₃ concentrations impact agricultural yields and nutritional quality of major crops (Ainsworth
1641 et al., 2012;Avnery et al., 2011), with consequences for global food security (Tai et al., 2014). Increasing
1642 background levels of O₃ are damaging to ecosystem health and reduce the global land carbon sink (Arneth et al.,
1643 2010;Sitch et al., 2007). Reduced uptake of carbon by plant photosynthesis due to O₃ damage allows more CO₂
1644 to remain in the atmosphere. This effect of O₃ on plant physiology represents an additional climate warming to
1645 the direct radiative forcing of O₃, a potent greenhouse gas (Collins et al., 2010;Sitch et al., 2007), the magnitude
1646 of which, however, remains highly uncertain (IPCC, 2013).”
1647
1648
1649 Lines 112-114: I find this a bit confusing - the authors discuss “high levels” and “elevated”
1650 ozone, but in the paragraph prior discuss mostly background concentrations. Can the
1651 authors
1652 make the transition a little smoother?
1653
1654 We have amended this, please see the paragraph above (Lines 113-120).
1655
1656 Lines 113: Please cut “future concentrations of ozone predicted for 2050”
1657
1658 This has been removed and replaced with (Line 135):
1659
1660 “The Wittig et al. (2007) meta-analysis of temperate and boreal tree species showed raised O₃ concentrations
1661 significantly.....”
1662
1663 Line 139: Here the authors refer to 46 ppb as “elevated” - in the previous sentences much
1664 higher concentrations are used. I would recommend just giving the concentrations, not
1665 qualifying them here and elsewhere
1666
1667 As recommended by the reviewer, we just give the concentrations of O₃ and do not qualify them (Lines 134 -
1668 148).
1669
1670 Line 153: What’s the time frame for Lombardozzi?
1671
1672 This has been added (Line 156):
1673

1674 “A second study by Lombardozzi et al. (2015) predicted a 10.8% decrease of present-day (2002-2009) GPP
1675 globally.”
1676
1677 **Line 194: please define ozone dose-response relationship**
1678
1679 We have modified this sentence as follows (Line 197-199):
1680
1681 “We make a separate distinction for the Mediterranean region where possible because the work of Bükér et al.
1682 (2015) showed that the sensitivity of dominant Mediterranean trees to O₃ is different to temperate species.”
1683
1684 We remove mention of dose-response relationships here as it is not necessary at this point, and these are
1685 introduced and defined later in section 2.2 lines 279 – 284.
1686
1687 **Line 220: I thought the authors re-arranged the supplementary figures to reflect the order
1688 they
1689 are mentioned in the text? This is the first occurrence of a supplementary figure and it’s
1690 figure
1691 S5.**
1692
1693 Apologies, this was an oversight and has now been changed.
1694
1695 **Line 227: of “stomatal ozone deposition”**
1696
1697 This has been modified (Line 231).
1698
1699 **Line 231-233: “because the impact of cumulative ozone exposure on plant productivity has
1700 already been calibrated with observations (described below)”**
1701
1702 This sentence has been changed (Line 234-236).
1703
1704 **Line 240: Can this be changed to interactive effects of CO₂ and O₃?**
1705
1706 This has been changed (Line 245).
1707
1708 **Line 225: Reference is missing the year - here and in line 332 - also I’m not sure why there
1709 is a
1710 comma before the parenthetical citation**
1711
1712 The citation references data downloaded from a web page. We have included the year the data was downloaded
1713 and removed the comma’s (Lines 332 - 339).
1714
1715 **Line 288: But how is the actually POD_y/ FO_{3crit} determined? Please specify here**
1716
1717 The values for POD_y/ FO_{3crit} are taken from the observation-based dose-response relationships. As to how
1718 these values are determined is a literature in itself and beyond the scope of this paper to describe here, so we
1719 refer the readers to the relevant papers (Line 294):
1720
1721 “For JULES, FO_{3crit} is the threshold for O₃ damage, and values for this parameter are taken from the O₃ dose-
1722 response relationships as the POD_y value (see CLRTAP, 2017 and Bükér et al. 2015 for derivation of POD_y
1723 values).”
1724
1725 **Line 298: Is “a” the ozone plant sensitivity? Please specify here**
1726
1727 This isn’t referring to the parameter ‘a’ here, so has been removed to stop confusion (Line 305). The parameter
1728 is always referred to as ‘a’.
1729
1730 **Line 302: It’s unclear to me how the authors incorporate the work of Bükér et al. from this**

1731 paragraph.
1732
1733 The work of B ker et al. (2015) shows that different O₃ dose-response relationships are needed to describe the
1734 O₃ sensitivity of dominant Mediterranean trees, so we use the different functions provided for Mediterranean
1735 trees instead of applying the function that has been derived dominantly from temperate/boreal tree species.
1736
1737 Line 380: The g₀ term has not previously been defined. I would just say a version of the
1738 Medlyn
1739 (2011) model that does not have an intercept
1740
1741 We amend the sentence as follows, as when there is no g₀ term the intercept is forced through zero (Line 387):
1742
1743 “The g_l parameter represents the sensitivity of g_s to the assimilation rate, i.e. plant water use efficiency, and was
1744 derived as in Lin et al. (2015) by fitting the Medlyn *et al.*, (2011) model to observations of g_s, photosynthesis,
1745 and VPD, assuming an intercept of zero.”
1746
1747 Line 416: “of” is missing. Can interaction be changed to interactive effects?
1748
1749 This has been changed (Line 423):
1750
1751 “.....to allow us to focus on the impact of O₃, CO₂ and their interactive effects.”
1752
1753 Line 431: phenology is misspelled
1754
1755 This has been changed (Line 439).
1756
1757 Lines 460-474: The point I wanted clarified here is that the agricultural mask does not
1758 change
1759 from 1900 to 2100
1760
1761 We have added the following sentence to clarify this point (Line 431 - 432):
1762
1763 “The agricultural mask is fixed and does not change over the simulation period.”
1764
1765 Lines 517 & 519: I don’t think an equation for the percentage change is necessary.
1766
1767 This has been removed (Line 524 - 528).
1768
1769 Figure S5 - Tg of N in b)? Tg Carbon in c)?, Gg of carbon in d)? Please specify. Are the NO_x
1770 numbers for anthropogenic sources or anthropogenic and natural? What about NMVOCs?
1771
1772 Units have been added to Figure S6.
1773
1774 Table 1 - One of the “O₃”s actually reads “O₂”
1775
1776 This has been changed.
1777
1778 Line 829: I would not say there are large improvements
1779
1780 ‘Large’ has been removed (Line 777).
1781
1782 Lines 841-855: A discussion of how incorporating ozone damage into JULES leads to a
1783 worse
1784 agreement with the MTE product & relevance for the authors’ work is needed here
1785
1786 We have added the following to the discussion (Lines 803-810):

1787 “In general, incorporating plant O₃ damage into JULES leads to worse agreement with the MTE GPP product,
1788 however, this is expected to some degree as we are adding an explicit representation of O₃ damage to a model
1789 calibrated to reproduce current day GPP and draw down of atmospheric CO₂. Inevitably this implicitly includes
1790 O₃ damage to vegetation. Explicit representation of plant O₃ damage is important to investigate how O₃ damage
1791 changes through time, under different emissions scenario’s, and the interactive effects with other gases (such as
1792 CO₂) and with climate change. The percentage changes we simulate are therefore important to demonstrate the
1793 sensitivity of modelled GPP and land Carbon to this process.”

1794
1795 Line 860-1: Can the authors give the time frame here? Does the range represent high vs.
1796 low
1797 sensitivity? Is this for O₃ +CO₂?

1798
1799 This sentence has been clarified (Line 814-815):

1800
1801 “Our estimates suggest O₃ (simulation O₃) reduced GPP by 2001 by 3% to 9% on average across Europe and
1802 NPP by 5% to 11% for the low and high plant O₃ sensitivities respectively (Table S3).”

1803
1804 Line 870: “Simulated ozone impacts will dependent on model ozone concentrations,
1805 meteorology, plant sensitivity to ozone, and process representation of ozone damage”

1806
1807 Thank you for the simplification! This has been changed (Line 823-825).

1808
1809 Lines 857-876: This section title is a bit of an oversell if the authors can’t explain the
1810 differences. How can the authors “expect” results if they end of concluding the studies are so
1811 different anyway?

1812
1813 We have changed the title of this section to (Line 812):

1814
1815 **“4.2 Comparison of modelled estimates of O₃ damage”**

1816
1817 Line 907: It seems like here the authors need to discuss the caveat that both high and low
1818 sensitivity simulations underpredict GPP

1819
1820 This has already been addressed in the discussion relating to the comparison of the JULES simulations to the
1821 MTE product (Section 4.1 Lines 787 to 808).

1822
1823 Lines 909-910: “may dampen”

1824
1825 This has been changed (Line 863).

1826
1827 Line 941: Can this be changed to interactive effects of O₃ and CO₂?

1828
1829 This has been changed (Line 970).

1830
1831 Line 884-886: please cut this discussion - the authors’ point is made - the information is
1832 lacking.

1833
1834 This has been removed (Line 902-905).

1835
1836 Line 888-908: The authors need to spell out the transition at the beginning of this paragraph

1837 —
1838 i.e., that another caveat of their study is that ozone is offline and the depositional sink is
1839 different here and in the model that was used to create forcing dataset. The comparison of
1840 the
1841 two gmax values is an apples-to-oranges comparison (one is model input, one is model

1842 output!) and I think it should be cut. I find the rest of the discussion not appropriate here - it's
1843 is
1844 already discussed in the methods. Please clearly state the caveat and cut most of this
1845 discussion (i.e., after Lines 891-908).

1846
1847 This paragraph has been changed as follows (Lines 908 - 915):

1848
1849 “A further caveat of this study is that the O₃ concentrations used to force the model are offline, in this case
1850 generated by the EMEP MSC-W model. This means the depositional sink is different in JULES (Medlyn
1851 formulation), compared to the EMEP model which uses the g_s formulation presented in Emberson et al. (2000)
1852 and Emberson et al. (2001). Because we link two different model systems, the g_s values in the EMEP model
1853 differ from those obtained using the Medlyn formulation, which would ultimately lead to different O₃
1854 concentrations. The role of EMEP in this study is to provide O₃ concentrations at the top of the vegetation
1855 canopy to force JULES and not g_s, how the different depositional sinks would affect simulated O₃
1856 concentrations at canopy height has not been investigated.”

1857
1858 Line 933-934: Why are the future tropospheric ozone concentrations highly uncertain?

1859 Future tropospheric O₃ concentrations will depend in a large part on how emissions of O₃ precursors change
1860 locally, regionally and globally. This is uncertain.

1861

1862

1863

1864